DISSERTATION

Submitted to
the combined faculties for Natural Sciences and Mathematics of the Ruperto-Carola University of Heidelberg, Germany for the degree of Doctor of Natural Sciences

Presented by
Chia-Hao Liu
born in Taipei, Taiwan

Date of oral examination: _____

Linkage analysis identifies an ubiquitin transferase gene as a novel marker for reduced quinine and quinidine responsiveness in *Plasmodium falciparum*

Referees: **Prof. Dr. Michael Lanzer**

Prof. Dr. Christine Clayton

Ich erkläre hiermit, dass ich die vorliegende Doktorarbeit selbstständig unter Anleitung verfasst und keine anderen als die angegebenen Quellen und Hilfsmittel benutzt habe.

Ich erkläre hiermit, dass ich an keiner anderen Stelle ein Prüfungsverfahren beantragt bzw. die Dissertation in dieser oder anderer Form bereits anderweitig als Prüfungsarbeit verwendet oder einer anderen Fakultät als Dissertation vorgelegt habe.

Die vorliegende Arbeit wurde am Department für Infektiologie, Abteilung Parasitologie des Universitätsklinikum Heidelberg in der Zeit von Januar 2009 bis Januar 2012 unter der Leitung von Prof. Dr. Michael Lanzer ausgeführt.

…….. ……

Datum Chia-Hao Liu

Acknowledgement

Three years sneaked off silently, I would like taking this opportunity to thank Prof. Dr. Michael Lanzer for letting me do this project in his laboratory and his supervision as well as his support and trust. I also acknowledge that Prof. Dr. Christine Clayton agreed to be the second examiner of my dissertation.

I am thankful to Prof. Wilfred D. Stein for his great help for and guiding me to the QTL world as well as all other collaborators who have contributed in this project and my Ph.D. dissertation. I also appreciate the participation of Prof. Dr. Christine Clayton, PD Dr. Ursula Klingmüller, and Dr. Ann-Kristin Müller in my Ph.D. dissertation defense committee.

I am especially grateful to Dr. Sybille Mayer and Dr. Astutiati Nurhasanah for their efforts in initiating this project and supervising me in the beginning of my study as well as Dr. Sanchez for providing me the constructs and her help for the figures. Among all the other lab members, I would like to thank Anurag, Alex, Anne, Sebastiano, Carorin, Carine, Sophia, Nicole, Martin, Miriam, Alessia, Ines, Katarina, Marina, Stefan, Elizabeth, Bianca, Dorothee, Luka, Petra, and Christian for their help and support during these three years.

In addition, I would like to thank Marie Curie Action for funding, and the InterMalTraining programme for the Ph.D. position, and Prof. Mike Blackman and Nathalie for organizing all the retreat and core course as well as all the administration stuff. I appreciate the support and courage from all the InterMalTraining students, Thomas, Maurice, Frank, Pradeep, Louise, Rhiannon, Caty, Serena, Eeshita, Sophie, Catherine, Shweta, and Marta.

I am also grateful to all my friends in Taiwan for their support and comfort , Biyin, Hualien_mouse, Yvan, Sorcery, and many friends in our military band.

I must thank my parents for their love and support, which let me still feel like home even though we are 10,000 km away. I also thank all my professors for training me during my bachelor (Tzu-Chi University) and master (National Taiwan University), especially Prof. Wen-Pin Wang and Nin-Nin Chuang, and encouraging me to pursue my Ph.D. degree.

Pascal Holzheu, my beloved, without your support and patience, I could not have done my Ph.D.

Abbreviations

A	Alanine
^{3}H	Tritium, tritiated
ABC	ATP Binding Cassette
ACT	artemisinin-based combination therapy
Amp	Ampicillin
AmpR	β-Lactamase gene for Ampicillin Resistance
APS	Ammonium persulphate
ATP	Adenosine Triphosphate
Bp	Base pairs
BSA	Bovine Serum Albumin
BLAST	Basic Local Alignment Search Tool
C	Cytosine or Cysteine
CAST	complexity analysis of sequence tracts
cDNA	complementary DNA
C-terminus	Carboxy terminus
CQ	chloroquine
D	Aspartic acid
dd H_2O	double distilled water
DEPC	Diethylpyrocarbonate
DIC	differential contrast image
DMSO	Dimethylsulfoxide
DNA	Deoxyribonucleic acid
DNAse	Deoxyribonuclease
dNTP	Deoxyribonucleoside triphosphate
E	Glutamic acid
E. coli	*Escherichia coli*
ECL	Enhanced chemiluminescence
EDTA	Ethylene Diaminotetraacetate
ER	Endoplasmic reticulum
ERAD	ER-associated degradation
EtBr	Ethidium bromide
et al	*et alii* (Latin) – and others

f	Femto
FWD	Forward
G	Glycine
g	Gram
GTP	Guanidine triphosphate
HECT	Homologous to the E6-AP Carboxyl Terminus
HEPES	N-(2-Hydroxylethyl)piperacin-N´-(2-ethylsulphonacid)
I	Isoleucine
IC_{50}	Half of maximal inhibitory concentration
IC_{90}	90% inhibition concentration
IFA	immunofluorescence assay
IPTG	Isopropyl β-D-1-thiogalactopyranoside
k	Kilo
K	Lysine
K76T	Threonine substitution to Lycine at amino acid 76
Kb	Kilobasepair
kDa	kilo-Dalton
L	Leucine
l	Liter
LB	Luria Bertani
LOD	logarithmic of odd
m	Milli
M	Molar or Methionine
$MgCl_2$	Magnesium Chloride
$MnCl_2$	Manganese Chloride
mRNA	messenger RNA
MR4	Malaria Research & Ref. Reagent Resource Center
n	Nano
N	Asparigine
N_2	Nitrogen
NBD	nucleotide binding domain
NCBI	National Center for Biotechnology Information
nm	Nanometers
O_2	Oxygen

°C	degree Celsius
O.D.	Optical density
P	Proline
P.	*Plasmodium*
PAGE	Polyacrylamide Gel Electrophoresis
PBS	Phosphate Buffered Saline
PBST	Phosphate buffered Saline supplemented with 0.1% Tween-20
PCR	Polymerase Chain Reaction
Pf	*Plasmodium falciparum*
pfcrt	*Plasmodium falciparum* chloroquine resistance Transporter coding sequence
*Pf*CRT	*Plasmodium falciparum* chloroquine resistance Transporter
pfmdr1	*Plasmodium falciparum* multidrug resistance protein 1 coding sequence
*Pf*MDR1	*Plasmodium falciparum* multidrug resistance protein 1
pfnhe	*P. falciparim* Sodium Hydrogen Exchanger coding sequence
*Pf*NHE	*Plasmodium falciparum* Sodium Hydrogen Exchanger
P-gp	P-glycoprotein
pH	Potential hydrogenii
PIPES	Piperazine-N,N′-bis(2-ethanesulfonic acid)
POD	Peroxidase
PV	Parasitophorous vacuole
PVDF	Polyvinyldifluoride
Q	Glutamine
QD	quinidine
QN	quinine
R	Arginine
RAMA	Rhoptry Associated Membrane Antigen
REV	Reverse
RFLP	Restriction fragment length polymorphisms

RING	Really Interesting New Gene
RNA	Ribonucleic acid
RNAse	Ribonuclease
rpm	revoluations per minute
RPMI	Rosewell Park Memorial Institute
S	Serine
SDS	Sodium dodecyl sulphate
SEM	Standard error of measurement
STS	Sequence Tagged Site
T	Threonine
TAE	Triacetate/EDTA
Taq	*Thermus aquaticus*
TE	Tris/EDTA
TEMED	triethylmethylethyldiamine
TMD	Transmembrane domain
Tris	tris (hydroxymethyl)-aminomethane
UT	putative ubiquitin transferase
UV	Ultraviolet
V	Volt or Valine
v/v	volume to volume
W	Tryptophan
w/v	weight to volume
WHO	World Health Organization
x	times or cross
X-ray	Roentgen ray
Y	Tyrosine
α	Anti
µ	Micro

Table of Contents

Abstract

The emergence and spread of drug resistance has complicated the clinical treatment of malaria, an infectious disease that caused about one million deaths in Africa annually. Chloroquine was the first-line treatment until 2001. Chloroquine resistance was detected simultaneously in the late 50's in all main endemic areas, spreading rapidly to South America and Africa. Thus, the use of chloroquine has had been discontinued. Chloroquine resistance mainly results from a K to T mutation at position 76 within the chloroquine resistance transporter, *pfcrt*. *Pfcrt* mutations have been reported to be involved in resistance to other quinoline drugs, including quinine. In the case of quinine there are evidences suggesting that reduced quinine susceptibility results from multiple mutational changes in genetic factors other than *pfcrt*. By analysis of quinine accumulation in the F1 progeny of HB3 x Dd2 genetic cross, previous studies have identified a novel quantitative trait locus on chromosome 7, termed B5M12 that synergistically interacts with *pfcrt* in reducing quinine susceptibility.

Subsequent analysis of 50 field isolates and lab strains could narrow down the locus to two candidate genes, including a putative ubiquitin transferase and RAMA (Rhoptry Associated Membrane Antigen). A Y to F mutation at position 1388 in the putative ubiquitin transferase was highly synergistically associated with mutant *pfcrt* in quinine resistance. The linkage analysis showed that Y1388F mutation of the putative ubiquitin transferase was co-selected with the *pfcrt* K76T mutation under the pressure of quinine treatment. RAMA was subsequently excluded as a candidate gene due to a lost of synergy with mutant *pfcrt* and the evidence that RAMA co-segregated with *pfcrt*. The identification of the putative ubiquitin transferase as a potential marker gene might improve the molecular surveillance of quinine resistance in the field. In addition, I also investigated the polymorphisms of *pfcrt* and *pfmdr1* in the 50 field isolates and lab strains. I could observe an additive effect of the geo-specific *pfcrt* M75E mutation in reduced quinine susceptibility. However, for *pfmdr1*, none of the mutation contributed to alter quinine susceptibility.

Zusammenfassung

Die Entstehung und die Ausbreitung von Medikamentenresistenzen hat die Behandlung von Malaria, einer Infektionskrankheit, welche mehr als eine Millionen Tote in Afrika verursacht, erschwert. Chloroquin war ab dem Zweiten Weltkrieg das wichtigste Medikament bei der Behandlung von Malaria. Allerdings trat in den späten 50iger Jahren Chloroquinresistenz in Südostasien auf, welche sich dann schnell nach Südamerika und Afrika ausbreitete. Deshalb wurde Chloroquin bald darauf abgesetzt. Chloroquinresistenz wird hauptsächlich durch eine Punktmutation von Aminosäure K zu T an Position 76 in dem *chloroquine resistance transporter*, *pfcrt*, verursacht. *Pfcrt*-Mutationen beeinflussen auch Resistenzen gegen andere Quinolinmedikamente wie zum Beispiel Chinin. Im Falle von Chinin gibt es Resultate, welche darauf hindeuten, dass Chininresistenz von mehr Faktoren beeinflusst wird als *pfcrt*. Durch Analyse der Chininakkumulation von den Nachkommen der genetischen Kreuzung zwischen HB3 und Dd2 in vorherigen Studien konnte ein neuer sogenannter "quantitative trait" Lokus auf Chromosom 7 identifiziert werden, B5M12. Der B5M12-Lokus interagiert synergistisch mit *pfcrt* bei der Reduzierung der Chininsuszeptibilität.

Durch eine nachfolgende Analyse von 50 Feldisolaten und Laborstämmen konnten wir den Lokus auf zwei Kandiadatengene eingrenzen: die Ubiquitintransferase und RAMA (Rhoptry Associated Membrane Antigen). Eine Y zu F Mutation an Position 1388 in der Ubiquitintransferase interagiert synergistisch mit mutiertem *pfcrt* bei Chininresistenz. Zusätzlich wurde unter Quininselektionsdruck durch Kopplungsanalyse die Ubiquitintransferase Y1388F mit *pfcrt* K76T co-selektiert. Im Anschluss daran wurde RAMA als Kandidatengen ausgeschlossen, aufgrund eines fehlenden Synergismus zu mutiertem *pfcrt* und des Trends der Zusammenlagerung mit *pfcrt*. Die Identifizierung einer möglichen Ubiquitintransferase könnte die molekulare Kontrolle der Quininresistenz im Feld verbessern. Zusätzlich haben wir die Polymorphismen von *pfcrt* und *pfmdr1* in 50 Feldisolaten und Laborstämmen untersucht. Wir konnten einen zusätzlichen Effekt der geospezifischen *pfcrt* M75E Mutation auf eine verringerte Quininsuszeptibilität zeigen. Im Fall von *pfmdr1* konnte für keine der Mutationen ein Einfluss auf die Quininsuszeptibilität gezeigt werde.

1 Introduction

1.1 Malaria overview

More than 40% of the world's population is at risk of contracting malaria, a mosquito-borne infectious disease. There are more than a million clinical cases of this disease, which causes 781,000 deaths annually in tropical and subtropical regions. Many of the affected geographical regions include much of Sub-Saharan Africa, Southeast Asia, and Latin America (WHO, World Malaria Report, 2010). The pathogen responsible for malaria is the protozoan parasite, *Plasmodium*, which has the following taxonomy: phylum Apicomplexa, class Sporozoa, order Coccidia, suborder Haemosporidiae, and family Plasmodiae. There are more than 100 species of *Plasmodium* parasites that are able to infect various animals, such as birds, reptiles, and numerous mammals. Human cases of malaria are primarily caused by four *Plasmodium* species, *Plasmodium falciparum*, *Plasmodium vivax*, *Plasmodium ovalae*, *Plasmodium malariae*, and *Plasmodium knowlesi*, which infect humans and its conventional host, macaques. *P. falciparum* is the malaria parasite that causes the majority of infections in Africa, and it is responsible for the most severe symptoms and mortality. *P. malariae* is found worldwide, whereas the least common malaria parasite is *P. ovalae*, which is restricted to West Africa. Both *P. ovalae* and *P. malariae* are relatively uncommon compared with *P. falciparum*. *P. vivax* is the geographically most widespread but is rarely fatal (Tuteja, 2007). *P. vivax* and *P. ovalae* are able to enter resting stages, known as the hypnozoite stage, in the liver. Hypnozoites cause a clinical relapse anywhere from months to four years following the initial infection (Greenwood, 2005).

Malaria is transmitted by *Anopheles* mosquitoes. Female mosquitos take blood meals to carry out egg production, and these meals are the link between humans and the mosquito hosts in the life cycle of *Plasmodium* species. The key regulatory factors of malaria transmission are temperature and humidity (higher temperatures accelerate parasite growth in the mosquito) and whether the Anopheles mosquitoes survive long enough to allow the parasite to complete its cycle in the mosquito. In contrast to the human host, the mosquito vectors do not suffer noticeably from the presence of the parasites.

There are 462 species of Anopheles mosquitoes throughout the world. Approximately 70 species have been shown to be natural human malaria vectors, and 39 species are the dominant transmitters of the majority of human malaria parasites (Hay et al., 2010).

1.2 Global malaria impact

Malaria is among the five leading causes of death due to infectious disease worldwide (following respiratory infections, HIV/AIDS, diarrhoeal diseases, and tuberculosis) and is the second leading cause of death from infectious diseases in Africa, after HIV/AIDS. Every 45 seconds, a child under 5 years old dies in Sub-Saharan Africa due to a malaria infection, accounting for 20 % of all childhood deaths in Africa (WHO, 2010).

The WHO World Malaria Report 2010 estimated that in 2009, approximately 3.28 billion people lived in areas that have low malaria transmission rates and that 1.2 billion people (one-fifth of world's population) lived in areas with high transmission rates. There were approximately 225 million clinical cases of malaria and 781,000 malaria-related deaths in 2009. Currently, malaria endemic regions encompass 106 countries. Eighty-one of these countries are focusing on malaria control, while 25 countries are in pre-elimination, elimination, or prevention of re-introduction phases. Morocco, the United Arab Emirates, and Turkmenistan have recently been certified as malaria-free countries. Figure 1.1 depicts the countries at risk of malaria transmission in 2010 (WHO, 2010).

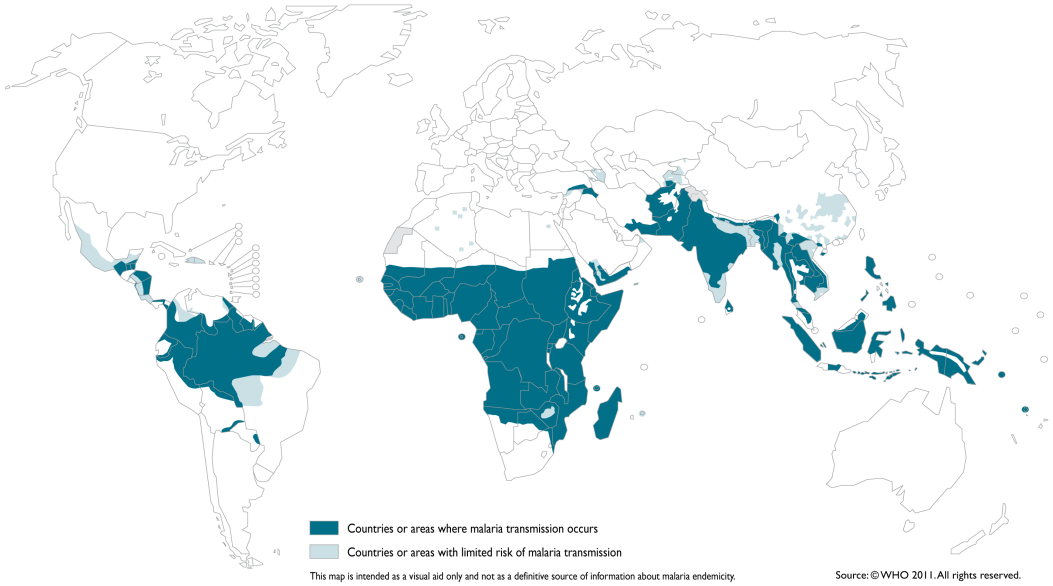

Figure 1.1 Countries or areas at risk of malaria transmission, 2010

People living in areas with high malaria transmission rates develop partial immunity to malaria within 10 to 15 years. However, during pregnancy, there is a transient depression of cell-mediated immunity that not only allows foetal allograft retention but also interferes with resistance to various infectious diseases (Uneke, 2007). In areas with high malaria transmission rates, women gain a level of immunity to malaria that becomes weaker during pregnancy. Malaria infection is more likely to contribute to maternal anaemia and delivery of low birth-weight infants (<2500 g or <5.5 pounds). Malaria is particularly problematic for women in their first and second pregnancies, for younger women, and for women who are HIV-positive. In areas with low malaria transmission rates, women generally do not develop immunity to malaria and are therefore more vulnerable to *Plasmodium* infection during pregnancy (Umbers et al., 2011). In 2009, 125 million pregnant women were at high risk of malaria infection, which resulted in approximately 200,000 infant deaths (Hviid et al., 2010).

In addition to mortality and morbidity, malaria is also commonly associated with poverty. It is indeed a cause of poverty and a major hindrance to economic development, especially in tropical endemic areas. People living in malaria endemic regions cannot afford prevention strategies or treatments against malaria. The economic impact of malaria has been estimated to be as high as $12 billion USD annually, and a reduction in annual economic growth was estimated at 1.3% (Greenwood, 2005). These economic impacts include the cost of health care, working days lost due to sickness, days lost in education, decreased productivity due to brain damage from cerebral malaria, and a loss of investments and tourism (Greenwood, 2005). In some countries with a heavy malaria burden, the disease may account for as much as 40% of public health expenditure, 30–50% of inpatient admissions, and 50% of outpatient visits (WHO, 2009). In addition, malaria jeopardises demographic transitions in Africa by causing high child mortality and infant mortality.

The cognitive abilities and school performances of malaria-infected children have been conclusively demonstrated to be impaired compared to those of healthy children. Comparisons of cognitive functions prior to and following treatment for acute malarial illness have shown significantly impaired school performances and cognitive abilities even following recovery. Malaria prophylaxis has been shown to improve cognitive function and school performance during clinical trials compared to placebo groups (Fernando et al., 2010).

1.3 Life cycle of *Plasmodium* species

The life cycle of malaria parasites is complex and involves two different hosts, the invertebrate Anopheles mosquito and another animal, for example a human. Malaria parasites in humans develop asexually in two phases, an exoerythrocytic (hepatic) and an intraerythrocytic phase. In Anopheles mosquitoes, the parasites undergo a transition from a sexual stage to an asexual stage. Figure 1.3 briefly depicts the life cycle of human malaria parasites.

During a single blood meal by Anopheles mosquitoes, thousands of sporozoites are released from the salivary gland of the mosquito. Sporozoites migrate rapidly through the human skin and into the bloodstream (Amino et al., 2006). Sporozoites subsequently migrate to the liver where they adhere to the endothelium of the sinusoid via receptors on the sporozoite surface, referred to as circumsporozoite proteins. The sporozoites then enter the liver by breaching the Kupffer cells and several hepatocytes before encountering a final hepatocyte host. (Frevert and Nardin, 2005; Mota et al., 2001). Subsequently, the entry of the sporozoite coincides with the formation of the parasitophorous vacuole, which originates from the hepatocyte plasma membrane. Within the hepatocytes, the sporozoites either remain dormant hypnozoites, which is only observed in *Plasmodium vivax* and *Plasmodium ovalae*, or they begin to divide via asexual replication into thousands of merozoites. The parasites then induce the detachment of the infected hepatocyte to migrate to the liver sinusoid. The parasite-filled merosomes then bud off from the hepatocyte, releasing approximately 10,000 to 30,000 merozoites into the blood stream. The length of the liver stage varies with *Plasmodium* species: 8-25 days for *P. falciparum*, 8-27 days for *P. vivax*, 9-17 days for *P. ovalae*, and 15-30 days for *P. malariae* (Tuteja, 2007).

The merozoites that are released into the blood stream evade the human immune system by invading and residing within erythrocytes. The invasion process is complicated and involves several phases; initial recognition and reversible attachment to the erythrocyte membrane; reorientation and formation of the junctions between the apical end of the merozoite (irreversible attachment); the release of the contents from the rhoptry and microneme;

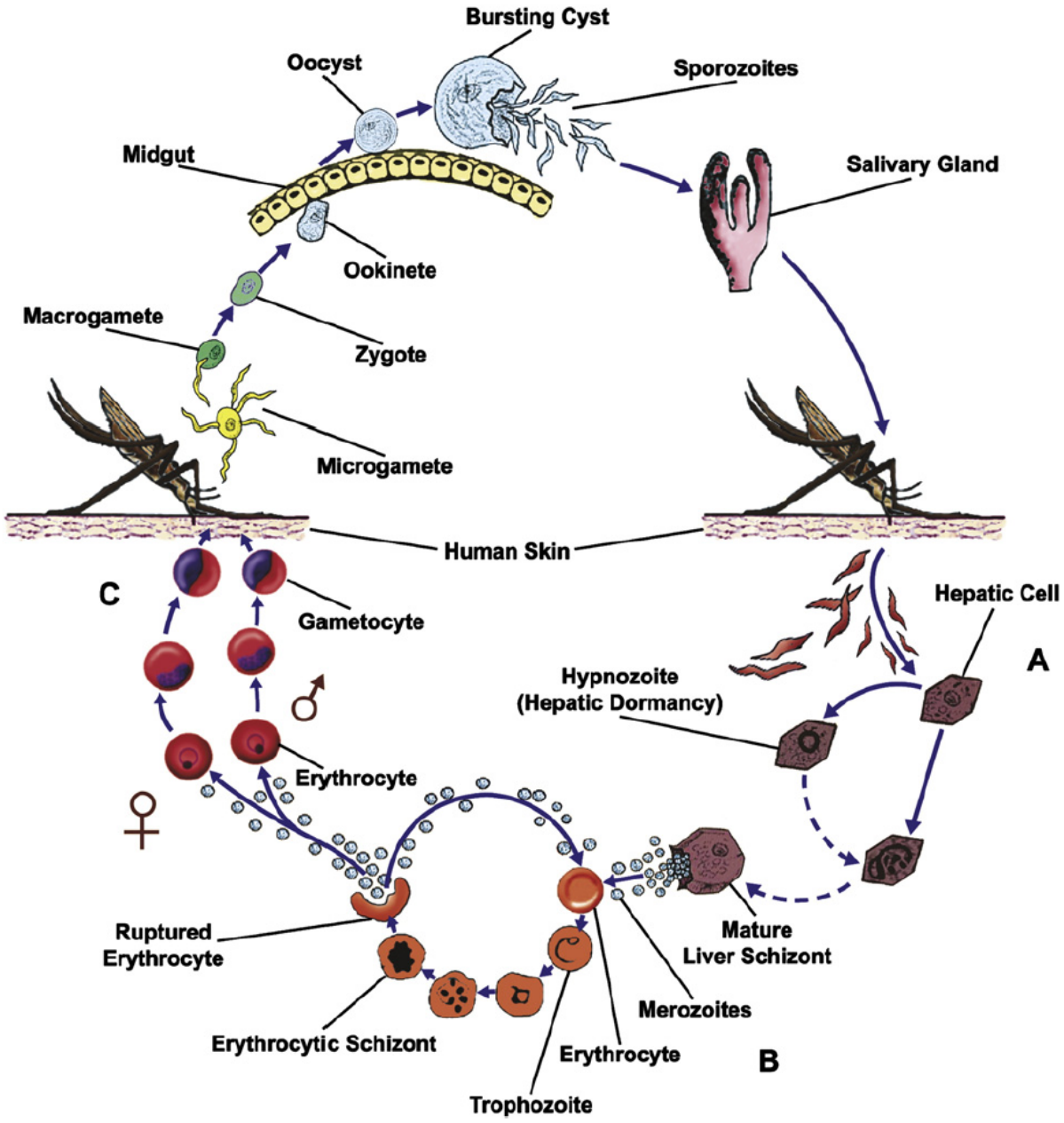

Figure 1.2 The life cycle of human malaria parasites (López et al., 2010).

formation of the parasitophorous vacuole; movement of the junction and invagination of the erythrocyte membrane surrounding the merozoite (accompanied by removal of the merozoite surface coat); and resealing of the parasitophorous vacuole and erythrocyte membranes following the completion of invasion (Miller and Greenwood, 2002). The merozoites rapidly invade the erythrocytes and replicate, causing the malarial symptoms of a fever and chill cycle.

During the blood stage, merozoites differentiate into trophozoites. The early trophozoite stage is also referred to as the ring stage due to the morphology of the parasite. The ring stage parasites substantially enlarge, an event that is accompanied by a highly active parasite metabolism, including the glycolysis of large amounts of imported glucose, the ingestion of erythrocyte cytoplasm, and the proteolysis of haemoglobin into its constituent amino acids. The mature trophozoites again undergo multiple rounds of nuclear division without cytokinesis, forming schizonts. Each mature schizont consists of approximately 20 merozoites, which are released following the bursting of the erythrocyte membrane. These merozoites subsequently invade uninfected erythrocytes. The erythrocytic cycle lasts approximately 48 hours in *P. falciparum*, *P. ovalae*, and *P. vivax* and 72 hours in *P. malariae*. Similar to the liver stage, the release of the merozoites coincides with a sharp increase in body temperature.

During the erythrocytic stage, some parasites transition into sexual stages, at which point they are referred to as gametocytes. Gametocytes are large single-nucleated parasites that fill the infected erythrocytes. Once the gametocytes enter the mosquito during a blood meal, they develop rapidly into mature male and female gametes and escape from the erythrocytes to fuse into a zygote, transitioning into the short-lived diploid ookinete stage. The motile and banana-shaped ookinetes migrate across the peritrophic matrix to the midgut of the mosquitoes, where they undergo multiple rounds of meiosis, forming an oocyst in the basal side of the midgut. Following multiple rounds of asexual replication, mature oocysts rupture and release large amounts of sporozoites into the haemocoel. From here, the sporozoites flow through the haemolymph and invade the salivary gland, waiting for the next bite to begin a new life cycle (Ersmark et al., 2006; Whitten et al., 2006).

1.4 Clinical manifestations

Malaria infection results in a broad variety of outcomes, including the absence of symptoms, mild to severe symptoms, and even death. Malaria can be categorised as uncomplicated or severe (complicated). All of the clinical symptoms are caused during the erythrocytic stage. While the parasites reside in the erythrocytes, numerous known and unknown waste substances, such as haemozoin pigments and other toxic factors, accumulate in the infected erythrocyte. These toxic compounds enter the blood stream following the burst of the infected erythrocyte and the release of invasive merozoites. These haemozoin pigments and other toxic factors, such as glucose phosphate isomerase, stimulate macrophage and other

immune cells to produce cytokines and other factors, resulting in fever, rigors, and likely the other severe pathophysiologies associated with malaria (Tuteja, 2007).

The period between the infective bite by the Anopheles mosquito and the presence of the first symptom is referred to as the incubation period. The incubation period of malaria varies with the parasite species: 7 days for *P. falciparum*, and up to 30 days for *P. malariae*. However, when diagnosed sufficiently early and treated correctly, malaria is generally curable.

1.4.1 Uncomplicated malaria

The classical malaria symptoms in uncomplicated cases last 6 to 10 hours, including a cold stage (a sensation of cold and shivering), which is followed by a hot stage (fever, headache, vomiting, and seizures in young children), and finally a sweating stage (sweating, normal temperature, and tiredness). Normally, the symptoms occur every second day with tertian parasites (*P. falciparum*, *P. vivax*, and *P. ovalae*) and every third day with the quartan parasite *P. malariae*. However, the egress of *P. falciparum* is often unsynchronised, resulting in a persistent spiking fever or daily fibril paroxysms (Rasti et al., 2004).

In addition to the above symptoms, patients may also present mild jaundice, increased respiration, perspiration, and an enlarged spleen and/or liver on physical examination (Tuteja, 2007; Miller and Greenwood, 2002).

1.4.2 Severe malaria

Severe malaria occurs when infections become complicated by serious organ failures or abnormalities in the patient's blood or metabolism. Severe malaria can include the following manifestations: abnormal behaviour, impaired consciousness, seizures, coma, or other neurological defects in cases of cerebral malaria; severe anaemia and haemoglobinuria due to haemolysis; and acute respiratory distress syndrome due to an inflammatory reaction in the lungs, inhibiting oxygen exchange and potentially occurring even after the parasite load has decreased in response to treatment. Other symptoms of severe malaria can include abnormalities in blood coagulation, low blood pressure, acute kidney failure, hyperparasitaemia (more than 5 %), metabolic acidosis, and hypoglycaemia, which also occurs in pregnant women with uncomplicated malaria or following quinine treatment (Miller, 2002).

1.5 Antimalarial compounds

Prescribing malaria treatment needs to be performed carefully with respect to the symptom severity, the species of malaria parasite, and the geographic location where the infection was acquired. The latter two factors aid in the determination of the probability that the parasite is resistant to certain antimalarial drugs. Other factors, such as the age, weight, and pregnancy status of the patient, may limit malaria treatment options.

A suitable antimalarial drug should be well-tolerated, safe, affordable and readily available in the endemic areas and have a short regimen. The most common antimalarial drugs, their targets, and their target life stages are listed in Table 1.1 (Kappe et al., 2010).

Table 1.1 Drugs and possible drug targets for drugs targeting erythrocytic-stage and liver-stage parasites. ES, Erythrocytic stage; LS, liver stage; DHFR, dihydrofolate reductase; DHPS, dihydropteroate synthase; SHMT, serine hydroxymethyltransferase (Kappe et al., 2010).

Taget function/ location	Drug	Life stage	Target
Apicoplast	Ciprofloxacin	ES and LS*	DNA replication
	Clindamycin/ doxycycline	ES and LS	protein translation
	Fosmidomyfin	ES and LS*	isoprenoid biosynthesis
	Rifampicin	ES and LS*	RNA transcription
	Fatty acid synthesis inhibitors	LS	fatty acid biosynthsis
Mitochondira	Atovaquone	ES and LS	cytochrome bc1 complex
Parasite cytoplasm	Pymethamine/ Chlorproguanil	ES	DHFR
	Sulfadoxine	ES	DHPS
	None	ES	SHMT
Endoplasmic reticulum	None	ES and LS*	plasmepsin V
Food vacuole	Chloroquine/ Amodiaquine	ES	heme polymerization
	Mefloquine/ Quinine	ES	heme polymerization
	Artemesnin‡	ES and gametocyte	heme polymerization
	None	ES	falcipains
	None	ES	plasmepsins
Parasitophorous vacuole	None	ES and LS*	putative translocon
Merozoite invasion	None	ES	rhomboid 4, subtilisin 2
Merozoite egress	None	ES and LS	DAPA3, SERA5, subtilisin 1
Unknown	Primaquine	LS and gametocytes	unknown

‡ Exact drug target is not known. *No published data to confirm drug action

Humans depend on the dietary intake of pre-formed dihydrofolate as an essential nutrient. Dihydrofolate is reduced to tetrahydrofolate, which is used in the biosynthesis of thymine, purine nucleotides, and several amino acids, such as methionine, glycine, serine,

glutamate, and histidine. However, malaria parasites can synthesise dihydrofolate from simple precursors and use exogenous dihydrofolate via a salvage pathway (Schlitzer, 2009). Antifolate compounds, such as pyrimethamine and sulfadoxine (Table 1.1), have been applied as an important antimalarial combination (also know as Fansidar) (Wiesner et al., 2003), though the rapid emergence of resistance has greatly reduced the efficacy of this drug (Yuthavong et al., 2006). Pyrimethamine and sulfadoxine show synergism against *P. falciparum*. The targets of pyrimethamine and sulfadoxine are dihydrofolate reductase (DHFR), the crystal structure of which has been determined (Yuvaniyama et al., 2003), and dihydropteroate synthase (DHPS), respectively. DHPS does not exist in humans, whereas plasmodial DHFR is structurally different from human DHFR. Thus, both enzymes are ideal for drug development. DHFR inhibition results in a reduction in tetrahydrofolate levels, decreasing glycine to serine conversion, methionine conversion, and lowering thymidylate levels. These events in turn arrest DNA replication (Gregson and Plowe, 2005).

Since the emergence of resistance to quinoline (see section 1.6) and the majority of antifolate drugs, artemisinin and its derivatives (artesunate, artemether, and dihydroartemisinin) have become important in malaria treatment. Artemisinin is an active ingredient from the qing hao weed (*Artemisia annua*), which has been used as a traditional Chinese medicine for hundreds of years to treat fever and several malaria symptoms (Shapiro et al., 2005). Artemisinin was first extracted and crystallised in 1971 (Woodrow and Krishna, 2006). Since then, semi-synthetic artemisinin derivatives with improved potency and bioavailabilities have been developed. Two hypothetical mechanisms of action of artemisinins in killing erythrocytic parasites have been reported (Eastman and Fidock, 2009; Schlitzer, 2009; Chaturvedi et al., 2010). First, artemisinins have a unique trioxane structure with an endoperoxide bond that is cleaved by reduced haem iron within the acidic digestive vacuole. The cleavage of artemisinin forms a free carbon radical, which is able to alkylate specific parasitic enzymes and inhibit the haem detoxification pathway, eventually killing the parasite. Secondly, the cleavage of artemisinin occurs in the cytoplasm of the parasite and is catalysed by a cytoplasmic Fe^{2+} source. The free radical acts specifically on *Pf*ATP6, which is related to the mammalian SERCA (sarcoplasmic endoplasmic reticulum calcium ATPase).

Artemisinins have the shortest half-life among all antimalarial drugs, approximately 0.5-1.4 hours. Among anti-malaria compounds, it is therefore the least likely that parasites will develop resistance against these drugs. However, the widespread monotherapy of artemisinins in Southeast Asia has reduced their efficacy and led to a delayed clearance of

parasites, especially on the Thai-Cambodia border (Dondorp et al., 2010). To prolong the efficacy of artemisinins, they are ideally administrated in combination with at least one other antimalarial drug, a practice known as artemisinin-based combination therapy (ACT) (Eastman and Fidock, 2009). The WHO has recommended ACTs as the first-line treatment for uncomplicated *P. falciparum* malaria since 2001. However, recent studies have reported the possible development of resistance to ACTs (WHO, 2010).

Several antibiotics known to be active against bacteria are also known to be effective against malaria parasites. These antibiotics interfere with the "bacteria-like" DNA replication, transcription, and translation in the parasite mitochondria and apicoplast. The mitochondrial genome is approximately 6 kb in length and encodes three proteins. However, in parasite mitochondria, many components required for translation must be imported from the cytosol. The apicoplast genome is approximately 35 kb in length and includes housekeeping genes involved in metabolic pathways. Antibiotics such as rifampicin are thought to block RNA synthesis in the apicoplast by inhibiting RNA polymerase; whereas tetracyclin, macrolides, and lincosamides are thought to inhibit protein synthesis in the apicoplast (Table 1.1) (Wiesner et al., 2003; Schlitzer, 2009).

1.6 Quinine

The first chemically synthesised and most commonly employed drugs for malaria treatment belong to quinine derivatives within the quinoline group. All of the quinine derivatives appear to interfere with haem sequestration. Despite the emergence of widespread drug resistance to certain quinoline antimalarial drugs, haem is still a viable target for novel antimalarial drug development (Wellems et al., 2009).

1.6.1 History—quinine, quinidine and chloroquine

The bark of *Cinchona officinalis* has been used to cure shivering by the Quechua Indians in Peru for centuries. The Quechua mixed the ground cinchona bark with sweetened water to cover the bitter taste of quinine. During the 17th century, malaria was endemic to Rome, resulting in numerous deaths of Roman popes and citizens. In 1640, the Jesuit brother Agostino Salumbrino, who received medical training in Lima, introduced cinchona bark to Europe to treat the shivering caused by malaria. Thus, cinchona bark was known as Jesuit's bark or Peruvian bark and became one of the most valuable goods shipped from Peru to Europe (Okombo et al., 2011). Prior to 1820, cinchona bark was first dried, ground to a fine

powder and mixed into wine for treatment. Beginning in 1850, people began to use cinchona bark as prophylaxis.

In 1820, the active compound (quinine) of cinchona bark was first isolated by Pelletier and Caventou, making malaria one of the first diseases treated with a pure substance (Wiesner et al., 2003). From 1860 to 1866, quinine and three other cinchona alkaloids (quinidine, cinchonine, and cinchonidine) were evaluated, which was one of the earliest clinical trials. The treatment of 3,600 patients indicated that all four compounds are comparable, with cure rates of over 98% (Achan et al., 2011). After 1890, quinine became the predominant antimalarial drug due to the massive Dutch and British plantations in Java (Indonesia), which produced approximately 22 million pounds of cinchona bark (97% of the world's quinine production).

In 1934, Andersag and his colleagues at Bayer Laboratory synthesised a novel 4-aminoquinoline compound N'-(7-chloroquinolin-4-yl)-N,N-diethyl-pentane-1,4-diamine, referred to as Resochin. The Germans ignored Resochin for a decade because it was considered too toxic for human use. During World War II, the allied powers were cut off from their supply of quinine because the Germans conquered the Netherlands and the Japanese controlled the Philippines and Indonesia. However, the United States had obtained four million cinchona seeds and planted them in Costa Rica. However, the planting of the cinchona tree was too late. Tens of thousands of U.S. soldiers in Africa and Southeast Asia died due to a lack of quinine. Thus, the U.S. government conducted clinical trials of other antimalarial drugs and unequivocally demonstrated that Resochin had significant therapeutic value. In 1947, Resochin, renamed chloroquine, was introduced for prophylaxis and routine treatment against malaria in all malaria endemic areas.

1.6.2 Haemoglobin metabolism and quinine and chloroquine mode of action

During the erythrocytic stage, malaria parasites ingest host haemoglobin via pinocytosis to meet their nutrient requirement and to counteract the osmotic imbalance caused by their own growth within the erythrocyte (Lew et al., 2004). The mechanism of haemoglobin transport into the digestive vacuole is unclear. Lazarous proposed that haemoglobin is transported primarily via cytosomes (Lazarou et al., 2009). However, Elliott suggested that haemoglobin transport is based on an internalisation mechanism of the host cell cytoplasm, one that is independent of actin polymerisation (Elliott et al., 2008).

Regardless of where the haemoglobin is digested, various proteolytic enzymes are involved in this degradation process, such as aspartic protease plasmepsin (Plm) I, II, and IV and the closely related histoaspartic protease (HAP), cysteine proteases (falcipain-1, -2, -2', and -3), the metalloprotease falcilysin, and dipeptidyl aminopeptidase 1 (DPAP1) (Ersmark et al., 2006).

The general haemoglobin metabolism pathway is illustrated in Figure 1.3. The precise order of cleavage in haemoglobin metabolism is unclear, especially whether a plasmepsin or falcipain catalyses the initial cleavage in the hinge region of the native haemoglobin tetramer linkage domain. The first cleavage unravels the protein to expose the regions of subsequent cleavages into small peptides. These cleavages are performed by both plasmepsins and falcipains. The metalloprotease falcilysin can only cleave small peptides (up to 20 amino acids), generating oligopeptides. DPAP1 was observed to cleave dipeptides from haemoglobin-derived oligopeptides in the digestive vacuole (Ersmark et al., 2006).

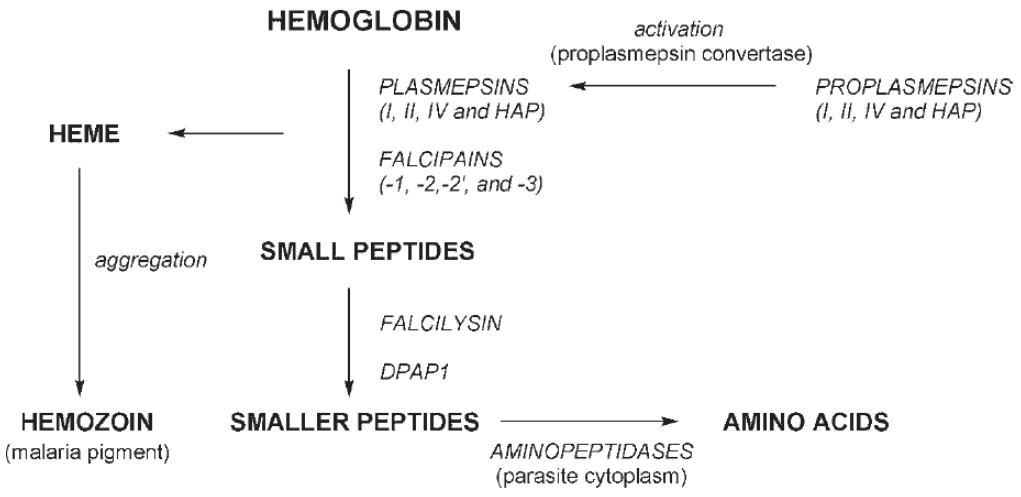

Fig 1.3 Haemoglobin metabolism in *Plasmodium falciparum* (Ersmark et al., 2006).

The products generated by the haemoglobin metabolic pathway are small oligopeptides and possibly free amino acids that are transported across the digestive vacuole membrane into the cytoplasm. However, the non-protein component of haemoglobin, haem (ferroprotoporphyrin), is not processed inside of the digestive vacuole. Haem is instead autoxidised to haematin (ferriprotoporphyrin), causing oxidative stress to the parasite. Haematin can bind to and disrupt cell membranes, damaging cell structures and lysing the host erythrocyte. The parasite deals with the toxic haematin by biomineralising this

compound into an inert and insoluble crystalline, β-haematin, also known as hemozoin or the malaria pigment. The hemozoin crystal is approximately 50-200 nm in length and contains approximately 80,000 haematin molecules. The formation of haemozoin is likely mediated by neutral lipid bodies (Egan, 2008; Coban et al., 2010; Pisciotta et al., 2007).

Although quinine has been used as an antimalarial drug for centuries, its mechanism of action is still not well understood. It is generally believed that the mechanism of action is similar to that of chloroquine, which can inhibit the biomineralisation of haem into haemozoin (Fig 1.4) (Petersen et al., 2011). Chloroquine is a weak base with pKa values of 8.1 and 10.2. Chloroquine is able to freely diffuse across several membranes as a free base. While in the acidic digestive vacuole (pH 4.5-5.2), chloroquine is trapped in its di-protonated form (Martin et al., 2009). Accumulated chloroquine binds to haematin, preventing the detoxification of haem (Fitch, 2004).

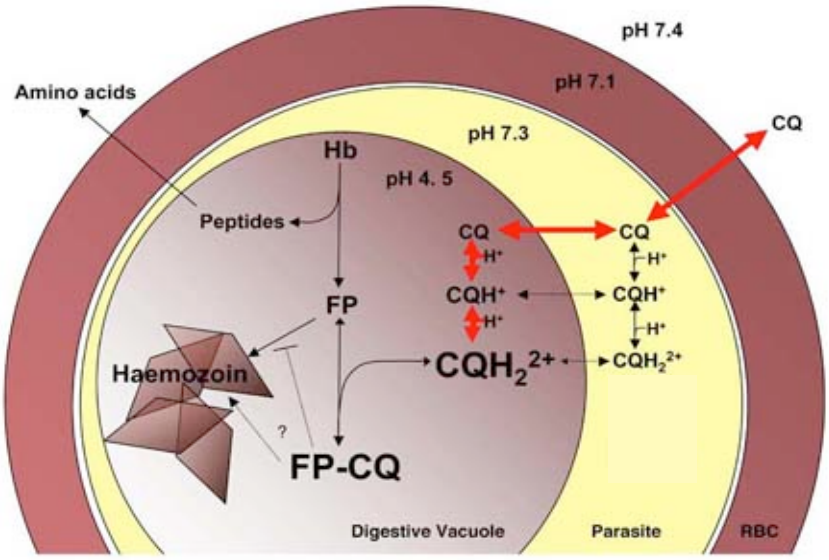

Fig 1.4 Chloroquine mechanism of action (Hladky, 2010). Chloroquine (CQ) diffuses through membranes into an acidic digestive vacuole, where CQ is protonated (CQH^+) or diprotonated (CQH_2^{2+}). CQ inhibits haemozoin biomineralisation by forming a complex with haematin (ferriprotoporphyrin, FP). Hb, Haemoglobin.

Similar to chloroquine, radiolabelled quinine can arrest growing haemozoin polymers in the presence of an inhibitor or plasmepsin I, which is responsible for the initial cleavage of haemoglobin (Mungthin et al., 1998). A recent study suggests that quinine forms an

intermolecular salt bridge with haem, interrupting the formation of the haematin dimer in the digestive vacuole. In addition, quantitative trait loci (QTL) analyses using quinine IC_{90} values and quinine accumulation have shown that quinine and chloroquine share at least one inheritable resistance determinant, *pfcrt*, the *Plasmodium falciparum* chloroquine resistant transporter (Ferdig et al., 2004).

1.6.3 Quinine and chloroquine resistance

In 1967, the WHO defined "drug resistance" as the ability of a parasite strain to survive or multiply despite the administration and absorption of a drug given in doses equal to or higher than those generally recommended but within the tolerance of the subject (WHO, 1967). Following World War II, chloroquine replaced quinine and was used extensively against malaria, resulting in the rapid development of chloroquine resistance. The first chloroquine-resistant parasite emerged in the Thai-Cambodian area. Resistance also emerged in Columbia 10 years following the introduction of chloroquine. Chloroquine resistance spread rapidly within 20 years from Southeast Asia to Africa and to new resistant foci, such as Papua New Guinea and the Philippines, in the late 1970s (Mita, 2009). To date, chloroquine resistant *P. falciparum* is predominant in nearly all malaria endemic areas (Petersen et al., 2011).

Due to the widespread use of chloroquine, quinine again began to play a key role in malaria treatment, including severe malaria, malaria in pregnancy and uncomplicated malaria (combined with other antibiotics). However, resistant *P. falciparum* has developed in Southeast Asia and perhaps in some African countries (clinical evidence not available). In addition, the efficacy of quinine remained for several decades in malaria endemic areas, which may be a cause of the high resistance of parasites to chloroquine (Okombo et al., 2010; 2011). Although the mechanisms of action of quinine and chloroquine are similar, quinine is still administered to treat malaria caused by chloroquine-resistant parasites, indicating that quinine resistance involves more factors than chloroquine resistance, which results from a K76T mutation in *pfcrt*. The putative molecular markers involved in quinine resistance are *pfcrt*, *pfmdr1*, and *pfnhe* (Mu et al., 2003; Ferdig et al., 2004).

Pfcrt was identified by analysing a genetic cross between a chloroquine-sensitive strain (HB3) and a chloroquine-resistant strain (Dd2); the resistance-mediating locus mapped

to the gene *pfcrt* (MAL7P1.27) (Su et al., 1999; Fidock et al., 2000). *Pfcrt* encodes a 45-kDa putative transporter, which consists of 10 predicted transmembrane domains and is located on the digestive vacuole membrane (Fig. 1.5). Different haplotypes *Pfcrt* are observed with respect to the geographic distribution of a given species. All of the mutations observed in chloroquine-resistant strains correspond to five origins of *pfcrt* mutants. Strains from Asia and Africa suggest a fitness cost of these mutations in that their prevalence has decreased

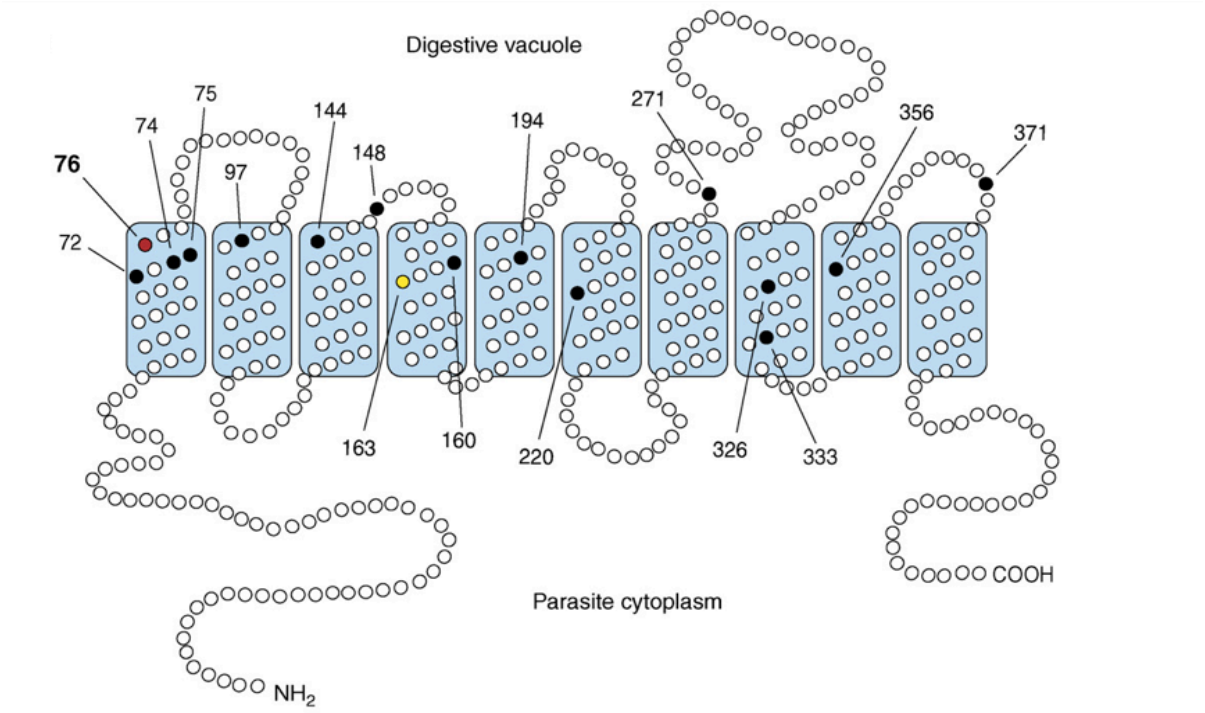

following the discontinuation of chloroquine administration (Table 1.2) (Hyde, 2005).

Figure 1.5 Topology and mutations in *pfcrt* (Valderramos and Fidock, 2006). The predicted topology of the 10 transmembrane domains of *Pf*CRT is illustrated, with the polymorphic residues marked.

The crystal structure and native function of *Pf*CRT remain unknown. *Pfcrt* homologs have been identified in several *Plasmodium* species (*P. vivax*, *Plasmodium yoelii*, *P. chabaudi*, *P. knowlesi*, and *P. berghei*). Other *Pf*CRT-like proteins have also been identified in several non-related organisms, such as *Arabidopsis thaliana.* A K76T mutation in pfcrt has been identified as the major determinant of chloroquine resistance through the use of allelic exchange experiments (Sidhu et al., 2002; Lakshmanan et al., 2005). The K76T mutation is also used as a genetic marker in molecular surveillance in several malaria endemic areas

(Petersen et al., 2011). Nonetheless, this mutation not only confers chloroquine resistance but also determines the level of susceptibility to other structurally related quinoline drugs, including quinine (Johnson et al., 2004; Ferdig et al., 2004). The *pfcrt* K76T mutation is highly associated with reduced chloroquine accumulation within the digestive vacuole in resistant strains (Cooper, 2007). However, in the case of quinine, reduced accumulation of quinine does not always correlate with increased quinine resistance (Sanchez et al., 2008a, 2011). The K76T mutation-mediated resistance to both chloroquine and quinine can be reversed by verapamil, which is used clinically as a calcium channel blocker, and inhibitors of drug efflux pump proteins, such as P-glycoprotein (Bellamy, 1996; Sanchez et al., 2008b). In addition to the K76T substitution, mutations affecting amino acids 74 and 75 can also alter chloroquine and amodiaquine susceptibility, effects that correspond to the differing geographic distributions of the mutant *pfcrt* alleles (Sá et al., 2009).

Table 1.2 *Pfcrt* allelic variants identified in P. falciparum field isolates and lab strains. Mutated residues are shaded in grey.

		PfCRT position and encoded amino acid														
Region	Reference line (origin)	72	74	75	76	97	144	148	160	194	220	271	326	333	356	371
	Chloroquine-sensitive															
All	Wild type (HB3, Honduras)	C	M	N	K	H	A	L	L	I	A	Q	N	T	I	R
	Chloroquine-resistant															
Asia and Africa	Dd2 (Indochina)	C	I	E	T	H	A	L	L	I	S	E	S	T	T	I
Southeast Asia	734 (Cambodia)	C	I	D	T	H	F	I	L	T	S	E	N	S	I	R
Pacific region	2300 (Indonesian Papua)	C	I	K	T	H	A	L	L	I	S	E	S	T	I	I
	PH2 (Philippines)	S	M	N	T	H	T	L	Y	I	A	Q	D	T	I	R
South America and Pacific	7G8 (Brazil)	S	M	N	T	H	A	L	L	I	S	Q	D	T	L	R

Gray shading indicates residues that differ from the wild-type allele.

TRENDS in Pharmacological Sciences

The second molecular marker that is often associated with quinine resistance is *pfmdr1* (*Plasmodium falciparum* multi drug resistance 1, *PF*E1150w) on chromosome 5. This gene encodes a 162 kDa protein, referred to as *Pf*MDR1 or Pgh-1, which belongs to the P-glycoprotein (P-gp) transporter of ATP-binding cassette (ABC) family. Similar to *Pf*CRT, *Pf*MDR1 is located on the digestive vacuole membrane and consists of two homologous dimers with 12 predicted transmembrane domains (Valderramos and Fidock, 2006) (Fig. 1.6). In bacteria and tumour cells, P-gp is often associated with verapamil-reversible multiple drug resistance given that the protein is capable of exporting several structurally and functionally unrelated cytotoxic agents (Borges-Walmsley et al., 2003; Valderramos and Fidock, 2006). In *P. falciparum*, *Pf*MDR1 imports the fluorophore Fluo-4 into the digestive vacuole, indicating

that *Pf*MDR1 may act as an active transporter of the digestive vacuole, sequestering cytotoxic metabolites and importing drugs (Rohrbach et al., 2006). In the same study, Rohrbach *et al*. demonstrated that quinine competes with *pf*MDR1-meditated Fluo-4 transport. In addition, exogenous expression of *Pf*MDR1 in *Xenopus* oocytes has indicated that this protein is able to transport antimalarial drugs in a selective manner. Wild type *Pf*MDR1 transports quinine and chloroquine but not halofantrine, whereas the mutant protein transports halofantrine but not

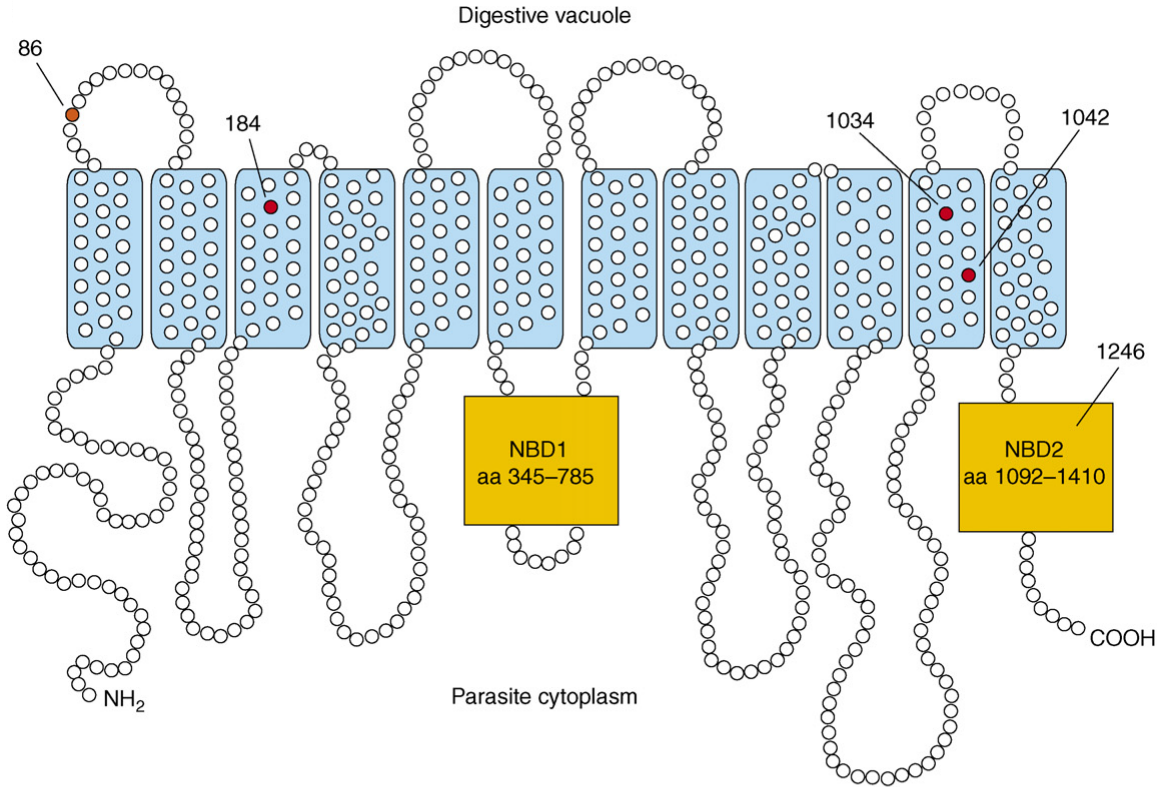

Figure 1.6 Topology and mutations in pfmdr1 (Valderramos and Fidock, 2006). *Pf*MDR1 consists two homologous dimers, each with six predicted transmembrane domains, and a nucleotide-binding pocket (NBD, shown in orange box) (Peel, 2001). Each NBD faces the cytoplasm of the parasite and binds to ATP.

Mutations in five residues (86, 184, 1034, 1042, and 1246) have been reported to be involved in altering the parasite's susceptibility to lumefantrine, artemisinin, quinine, mefloquine, halofantrine and chloroquine (Table 1.3) (Petersen et al., 2011). The N1042D substitution appears to play a role in quinine resistance (Sidhu et al., 2005). Amplification of *pfmdr1* is also associated with reduced susceptibility to lumefantrine, artemisinin, quinine, mefloquine, and halofantrine, while a reduction in *pfmdr1* copy number results in increased chloroquine resistance (Barnes et al., 1992; Anderson et al., 2009). In addition to mutations

and copy number polymorphisms, nuclear-receptor-mediated responses to drug exposure may be a mechanism of gene regulation in *P. falciparum* (Johnson, 2008).

Table 1.3 *Pfmdr1* allelic variants identified in P. falciparum field isolates and lab strains. Mutated residues are shaded in grey.

		PfMDR1 position and amino acid					Copy number
Region	Reference line (origin)	86	184	1034	1042	1246	
All	Wild type (3D7, Netherlands)	N	Y	S	N	D	1
Asia and Africa	FCB (Southeast Asia)	N	Y	S	N	D	≥2
	K1 (Thailand)	Y	Y	S	N	D	1
South America	7G8 (Brazil)	N	F	C	D	Y	1

Gray shading indicates residues that differ from the wild-type allele.

TRENDS in Pharmacological Sciences

The third molecular marker implicated in reduced quinine susceptibility is a Na^+/ H^+ exchanger (*pfnhe*, *PF*13_0019), which encodes a 226 kDa protein located on the parasite's plasma membrane. This protein has 12 predicted transmembrane domains (Bennett et al., 2007). The complete function of *Pf*NHE remains unknown, but it has been speculated that *Pf*NHE maintains the parasite's neutral pH (7.4) (Bosia et al., 1993). However, later studies have shown that the neutral pH within the parasite is maintained by a plasma membrane V-type H^+-ATPase (Spillman et al., 2009). An increase in the number of DNNND repeats has been proposed to be associated with decreased quinine susceptibility (Henry et al., 2009; Okombo et al., 2010; 2011). In field studies, however, the association between *pfnhe* and reduced quinine response has been questioned (Briolant et al., 2011; Andriantsoanirina et al., 2010). Nevertheless, biochemical analyses have demonstrated that reduced expression of *Pf*NHE as a result of a truncated *pfcrt* promoter results in significantly reduced quinine susceptibility *in vitro* (Nkrumah et al., 2009).

In addition to *pfcrt*, *pfmdr1* and *pfnhe*, recent studies have identified a multidrug resistance-associated protein (*Pfmrp*, *PF*A0590w) as a contributor to drug resistance. *Pfmrp* belongs to the ABC transporter C subfamily, which is known to transport anion-like glutathione (GSH), glucoronate, and various drugs. *Pf*MRP is located on the plasma membrane and membrane-bound vesicles within the parasites. *Pf*MRP is not essential during the erythrocytic stage, but its deletion results in increased susceptibility to chloroquine, quinine, artemisinin, piperaquine and primaquine. Deletion of this gene also results in the

accumulation of GSH, chloroquine and quinine (Raj et al., 2009). Previous linkage studies based on *in vitro* drug susceptibility assays in field isolates have demonstrated that two point mutations (Y191H and A437S) reduce quinine and chloroquine susceptibility (Mu et al., 2003). However, *pfmrp* is presumably not the major determinant of antimalarial drug resistance, and *Pf*MRP possibly acts with other transporters to efflux drugs and other metabolites out of the parasites (Raj et al., 2009).

Previous studies have identified several putative genetic markers that have been proposed to play a role in quinine resistance (Mu et al., 2003; Raj et al., 2009; Ferdig et al., 2004). Interestingly, all of these molecular markers encode various transporters, indicating that quinine resistance is associated with reduced intracellular quinine accumulation. Following up on this hypothesis, two former Ph.D. students in our laboratory performed QTL analyses on susceptibility to quinine and its stereoisomer quinidine and on the initial and steady-state intracellular drug accumulation levels in the F1 progeny of HB3 and Dd2 genetic crosses (Mayer, 2009; Nurhasanah, 2009).

1.7 QTL analyses of quinine and quinidine accumulation

To determine the mechanism of quinine resistance, former Ph.D. students in our lab measured the time-course of quinine and quinidine accumulation in the parental strains Dd2 (quinine sensitive) and HB3 (quinine sensitive) according to a previously described method (Sanchez et al., 2003). Quinine accumulation is given as the ratio of the intracellular to extracellular quinine concentration. The Dd2 strain accumulates a low amount of quinine, whereas HB3 accumulates approximately twice as much quinine as Dd2. Two time points were selected for the following studies: 5 minutes for the initial uptake phase and 20 minutes for the saturated uptake phase.

Subsequently, they measured quinine and quinidine accumulation in the 34 F1 progeny of the Dd2 x HB3 genetic cross. Variations were observed in the quinine and quinidine accumulation levels among the progeny; some progeny accumulate quinine and quinidine at a level comparable to the parental strains, whereas others exhibit intermediate or higher levels of accumulation. This finding indicates that multiple genetic factors may be involved in quinine/quinidine accumulation, which is consistent with previous studies indicating that quinine resistance is multifactorial (Mu et al., 2003; Ferdig et al., 2004; Raj et al., 2009).

Previous QTL analyses of quinine IC_{90} values in the F1 progeny of Dd2 x HB3 genetic crosses identified three genetic markers that are associated with reduced quinine susceptibility: *pfcrt, pfnhe,* and *pfmdr1* (Ferdig et al., 2004). In our group, former Ph.D. students performed QTL analyses of quinine and quinidine accumulation. These analyses identified a bifurcated peak on chromosome 7 that is highly associated with quinine and quinidine accumulation. The downstream locus contains *pfcrt*, and the upstream locus is termed B5M12 (the central microsatellite marker of the locus). The B5M12 locus was further investigated to compare the results with those of the previous analyses of quinine IC_{90} values performed by Ferdig et al. in 2004. It was observed that the logarithmic odd (LOD) score of the B5M12 locus is significant for the QTL analyses of quinine IC_{90} values ($p < 0.01$). However, the LOD score of the B5M12 locus was higher in QTL analysis of quinine accumulation than for quinine IC_{90} values, suggesting the QTL analysis of quinine accumulation is a more sensitive technique for investigating quinine resistance. With respect to quinidine, QTL analyses of both accumulation and IC_{50} data (provided by Dr. Ferdig) gave similar results, i.e., both analyses returned a bifurcated peak including *pfcrt* and the B5M12 locus. In addition, QTL analyses of quinine IC_{90} values revealed a second peak on chromosome 13. This peak contained the *pfnhe* gene and was not observed in the quinine accumulation QTL study, indicating that *Pf*NHE may be the drug target or involved in the parasite's clearance mechanism (Mayer, 2009; Nurhasanah, 2009).

To investigate the contribution of *pfcrt* and the B5M12 locus to quinine and quinidine accumulation, they grouped the quinine and quinidine accumulation and susceptibility values of the 34 F1 progeny according to the parasites' *pfcrt* and B5M12 haplotypes. No significant difference was observed between the progeny that possess both loci inherited from HB3 and the progeny possessing either *pfcrt* or the B5M12 locus inherited from Dd2, indicating that no loci alone is able to confer the reduced quinine or quinidine accumulation phenotype. It is only when the progeny possess both loci inherited from Dd2 that the parasites have significantly reduced quinine and quinidine accumulation, suggesting that these two loci interact synergistically in reducing quinine and quinidine accumulation (Mayer, 2009; Nurhasanah, 2009).

When they performed the same grouping using data from quinine and quinidine *in vitro* drug susceptibility analyses (i.e., quinine IC_{90} values and quinidine IC_{50} values from Ferdig's group), both loci were observed to be required for reduced accumulation of quinine and quinidine; the remaining contribution is conferred by the two loci on chromosome 13.

Therefore, the synergy between *pfcrt* and the B5M12 locus appears to genetically characterise the altered quinine and quinidine responsiveness of these strains (Mayer, 2009; Nurhasanah, 2009).

Patel *et al*. recently re-investigated the chloroquine responsiveness in the HB3 and Dd2 genetic cross and noted a possible contribution of the B5M12 locus in addition to *pfcrt*. To further elucidate the interaction of *pfcrt* and the B5M12 locus to chloroquine responsiveness, they performed a grouping of three different data sets of chloroquine IC_{50} values from HB3 x Dd2 genetic crosses. These data were collected from Patel et al. (2010), Sá et al. (2009), and their own study. In addition, they analysed chloroquine accumulation. *Pfcrt* alone, independently of the B5M12 locus, confers significantly decreased chloroquine accumulation and reduced chloroquine susceptibility. However, the B5M12 locus only appears to act additively with *pfcrt* in terms of reduced chloroquine susceptibility in the data set from Patel *et al*., but this conclusion was not reached for other datasets. Thus, the contribution of B5M12 to chloroquine responsiveness is quite different from its contribution to quinine and quinidine responsiveness, where both *pfcrt* and the B5M12 locus are required to confer reduced responsiveness (Mayer, 2009; Nurhasanah, 2009).

The B5M12 locus is approximately 185 kbp long and contains 40 genes. There are 4 genes encoding tRNAs were excluded from the following study. Further studies are necessary to dissect the properties of the B5M12 locus and to identify novel genetic markers of quinine resistance therein.

It has been shown that reduced *Pf*NHE expression as the result of truncated *pfcrt* promoter results in significantly reduced quinine susceptibility (Nkrumah, 2009). However, neither quinine nor quinidine accumulation in *Pf*NHE mutants is significantly reduced when compared with wild type, indicating that *Pf*NHE may be a target of quinine and quinidine or involved in the process of parasite clearance (Mayer, 2009).

1.8 Aim of Study

The aim of this thesis was to dissect this B5M12 locus and identify gene(s) contributing to quinine resistance in *P. falciparum*. The associations of other polymorphisms in known molecular markers with quinine resistance were also investigated. A better understanding of the genetic bases of quinine resistance will be able to improve the molecular surveillance of quinine resistant parasites in the endemic areas and may help preserve this valuable antimalarial drug.

2 Materials and Methods

2.1 Materials

2.1.1 Equipments

Analytical scales	Sartorius, Göttingen
Autoclave	Tuttnauer Systec 2540, Wettenberg
Centrifuges	
Biofuge fresco	Heraeus Instruments, Hanau
Biofuge pico	Heraeus Instruments, Hanau
J2-MC	Beckman, Krefeld
L-60 Ultracentrifuge	Beckman, Krefeld
Megafuge 1.0 R	Heraeus Instruments, Hanau
Megafuge 2.0 R	Heraeus Instruments, Hanau
RC5BPlus	Sorvall, Langenselbold
Computer Software	
Adobe Photoshop ®5.0	Adobe Systems Inc, USA
EndNote 8.0.	ISI Research Soft, CA, USA
Internet Explorer	Microsoft Corporation, USA
MS Powerpoint 2011	Microsoft Corporation, USA
MS Word 2011	Microsoft Corporation, USA
SigmaPlot 11.0	Systat Software Inc.
BioEdit 7.08	Ibis bioscience, USA
PyroMark IdentiFire SW 1.0	QIAGEN®
Swiss-PdbViewer 4.04	Swiss Institue of Bioinformatics
DNA-electrophoresis apparatus	Biorad, München
Freezer -80°C, UF85-300S	Heraeus GmbH, Hanau
Freezers -20°C	Liebherr, Biberach
Fridges	Liebherr, Biberach
Gas burner gasprofi 1 micro	WLD-TEC
Glass capillaries GB100F10	Scientific products GmBH, Germany
Ice machine AF 30	Scotasman, Milano, Italy

Incubator (*P. falciparum*)	Heraeus GmbH, Hanau
Incubator (bacteria)	Heraeus GmbH, Hanau
Liquid nitrogen tank	Air Liquide, Ludwigshafen
Magnetic stirrer	Heidolph, Schwabach
Microscopes	
Light optical microscope	Zeiss, Jena
Leica DMII	Leica
Confocal laser-scanning microscope	Zeiss, Jena
Microwave oven	AEG, Nürnberg
PCR machine	
T gradient Thermocycler	Biometra, Göttingen
GeneAmp PCR system 9700	Applied Biosystems, USA
pH-Meter pH 537	WTW, Weilheim
Pipetman Gilson P10, P20, P1000	Abimed, Langenfeld
Multipipetman	Abimed, Langenfeld
Pipetus-akku	Hirschman labortechnik, Eberstadt
pipetus® standard	Hirschman labortechnik, Eberstadt
Power supply: Power Pac 300	Biorad, München
PyroMark™ Q96 ID	QIAGEN®
Rotor JA20.1	Beckman instruments, USA
Rotor SS-34, GS-3, SM24	DuPont Instruments, Bad Homburg
Spectrometer UVIKON 923	Kontron Instruments
Sterile work bench Herasafe	Heraeus Instruments, Hanau
Stopwatch	Roth, Karlsruhe
Trans-blot® SD Semidry transfer cell	Biorad, München
Tweezers	Dumont, Switzerland
UV-table UV –Transilluminator	Gibco BRL, Karlsruhe
VarioMACS, MACS system	Miltenyi Biotec, Bergisch Gladbach
Vortex Genie 2	Roth, Karlsruhe
Watherbath Julabo 7A	Julabo Labortechnik, Seelbach

2.1.2 Disposables

Aluminium foil	Roth, Karlsruhe
Amicon Ultra Centrifugal Filter Devices MW 30, 50 ml	Millipore Corp., Billerica, USA

Centrifuge tubes, Polypropylene 18/95	Greiner Bio-one, Frickenhausen
Clingfilm Saran	Dow Chemical Company, Schwalbach
Cuvettes	Saarstedt, Nümbrecht, Germany
Eppendorf tubes	Saarstedt, Nümbrecht, Germany
Falcon tubes (15 ml, 50 ml)	Corning incorporation, Bode*nhe*im
Gloves	Harmann, Heide*nhe*im
Immersion oil	Zeiss, Jena
Kimwipes lite 200	Kimberly Clark
MACS-column CS	Miltenyi Biotec, Bergisch Gladbach
Parafilm	Americal International CanTM, USA
PCR softtubes 0.25 ml	Biozym Scientific GmbH
Petri dishes (10 ml diameter)	Greiner Bio-one, Frickenhausen
Petri-dishes (25 ml diameter)	Greiner Bio-one, Frickenhausen
Pipette Tipps	Corning Inc, Bode*nhe*im
Plastic pipettes (1 ml; 2 ml; 5 ml; 10 ml; 25 ml)	Corning Inc. Bode*nhe*im
PVDF Membran 0.45 µm	Millipore Corp., Billerica, USA
Sterile filters (0.2 and 0.45 µm)	Millipore GmbH, Ashburn
Stiches	
Sterile filtration devices	Corning incorporation, Bode*nhe*im
Thermowell PCR tubes	Corning incorporation, Bode*nhe*im
WhatmanTM 3 mm Paper	Whatman Paper Company
X-ray film	Kodak

2.1.3 Chemicals

The chemicals for the purpose of this study were purchased from the firms Roth, Merck, Sigma, Serva, Applichem, and GE Healthcare. These were either ordered directly or through the chemicals facility of the University of Heidelberg medical school.

2.1.4 Kits

Gel extraction kit	QIAGEN®
PCR purification kit	QIAGEN®
High pure plasmid miniprep Kit	Roche, Man*nhe*im
DNeasy Blood & Tissue Kit	QIAGEN®
SuperScript® III First-Strand Synthesis SuperMix	Invitrogen, USA
Enhanced Chemiluminescence kit	Pierce® , U.S.A.
pyroMark Gold Q96	QIAGEN®

2.1.5 Biological Materials

2.1.5.1 Size markers and loading buffers

6 x DNA loading buffer	Fermentas, Germany.
GeneRuler 1 Kb DNA ladder plus	Fermentas, Germany.
2x Protein loading buffer	
PageRuler Plus Prestained protein ladder	Fermentas, Germany.

2.1.5.2 Enzymes

EuroTaq polymerase	BioCat GmbH, Heidelberg, Germany.
Phusion Polymerase	Fermentas, Germany.
Restriction Enzymes	New England Biolabs
DNase I	Roche, Man*nhe*im
Lysozyme	Roche, Man*nhe*im

2.1.5.3 Plasmid

pET28a(+) Novagen, Darmstadt

2.1.5.4 *E. coli* strain

BL21(DE3) (Stratagene)

2.1.5.5 Antibodies

α-6 x His Mouse monoclonal antibody (1:1000) Novagen, USA

Ubiquitin transferase polyclonal antibody

Rabbit α –mouse IgG POD	Dianova, Hamburg
Goat α-mouse IgG Alexa 488	Dianova, Hamburg

2.1.5.6 Animal

NMRI mouse	Charles River, USA

2.1.5.7 Parasite strains

Parasite strains used in this study were obtained from the Malaria Research and Reference Reagent Resource Center (MR4), USA.

3D7	chloroquine sensitive strain
Dd2	chloroquine resistant strain
HB3	chloroquine sensitive strain
7G8	chloroquine resistant strain
GB4	chloroquine resistant strain

Table 2.1 Field Isolates and their origin.

The genomic DNA of field isolates was kindly provided by Dr. Mu Jiangbing from NIAID.

Strain	Origin	Strain	Origin
1088	Thailand	Thai18	Thailand
CP250	Cambodia	CP305	Cambodia
CP313	Cambodia	CP285	Cambodia
CP297	Cambodia	CP252	Cambodia
Thai2	Thailand	CP203	Cambodia
713	Guinea Bissau	PNG9-1	Papua New Guinea
CP201	Cambodia	CP269	Cambodia
CP238	Cambodia	P31	Thailand
98-18	Thailand	DIV14	Brazil
98-5	Thailand	DIV17	Brazil
ECP	Brazil	98-11	Thailand
PBZ945	Brazil	M97	The Gambia
CP256	Cambodia	PBZ357	Brazil
Thai-19	Thailand	FCR3	Thailand
9021	Ghana	PAD	Brazil
99-18	Thailand	DIV30	Brazil
ICS	Brazil	CP271	Cambodia
98-17	Thailand	K39	Kenya
IF4/1	Liberia	REN	Sudan
102/1	Sudan	Camp	Malasya
418	Gambia	M24	Kenya
FAB6	South Africa	92-9	Thailand
M5	Mali		

2.1.5.8 Oligonucleotides

The oligonucleotides (primers) used in this study were ordered from Thermo Electron GmbH (Ulm).

Table 2.2 Primers for sequencing the genes located in the B5M12 locus. These primers were used for identification of polymorphisms in HB3 and Dd2, and subsequently in field isolates.

Gene	Primers	Position	Sequences (5' to 3')
MAL7P1.16	FWD_7	224590	CAA GAG CAA CAC AAA TTA TTA AC
	REV_7		GCT TAG TAC GGA AAA TAT TCT C
	FWD_6	225853	GTA AAC CCT TTT GTG GTT TAT C
	REV_6		GAA GTA TTC ATA CTT CTC AAG G
	FWD_5	226815	CTG TTT TGT TTA TGA GGA TAA G
	REV_5		TGG AAA GGA CCT AAA CTT TTC
	FWD_4	227954	GTA CAT GTA GAA AAT ATA AAC C
	REV_4		CTA TCC ACA TCT TCA TCA GC
	FWD_3	229643	CAT GGG TTA TTA TGG TGT CC
	REV_3		CAA TAT TGT GGA ATT TAT CTG TG
	FWD_2	231209	CCG ACA ATT CAT TAA GAT ACC
	REV_2		CTT TCA ATC GTT TGG CTA GC
	FWD_1	232282	GAG CCG TAT AAA TTG TAA GAG
	REV_1		GTG ATG TAC ATT AAT CAT AAA TG
MAL7P1.17	FWD_1	235419	CAC CAG CAC CAC CGA CTC
	REV_1		GAA AAG GAG AAG ATC ATA AAT AC
	FWD_2	236170	GTA TCT TCA AAT ATA AAA ACA GAA C
	REV_2		CTT TTC TTT TTA ATA AGA GTT CTT G
	FWD_3	238180	GAG CTT AAT ATT CAT CAG GAT G
	REV_3		CCC CTT CAA TTT ATT CGA GTC
	FWD_4	239343	CTA TAC TGT ATT TCA AGA TAG TAC
	REV_4		CAT GTC TTC TAA ATG TTG TAT ATC
	FWD_5	241382	CGG AAG AAC AAA GTA TTT ATA CG
	REV_5		CGT TGT TTT GTG TTA TCT TAT TTG
	FWD_6	242588	GTA TTC CAT ACA ATA ACA AAT ATG
	REV_6		CAG TAA AAT ACG AAT TTA GTG AC
	FWD_7	244062	CTT AAT CTT CGG AAG TAA TTA C
	REV_7		CTA TGT CTA CTT GAA TCC TTC
	FWD_8	245038	GAT AAT TAT GAG CAT ATA CTA AAC
	REV_8		CGA ACA TAT GTT CAC TTG TAT C
*PF*07_0015	FWD_3	247896	GCA ACA TTC TAG ATT TTG AAT AC
	REV_3		CCA CTT TTA TTA AAT CTA ATA TTA C
	FWD_2	249086	GAA AAT TCA AAC TTG GAA AAT AAT G
	REV_2		CAA CTT ATG TGT ATT ACC ATT ATC
	FWD_1	250242	ATG GAA AAC GAT AAA CAA AGT AAC
	REV_1		CCT TTG TTA ATT CAA TGG ATC TC
	REV_1B		GTA GCA TAC TAA CAA GTT CTT GTC

Gene	Primers	Position	Sequences (5' to 3')
*PF*07_0016	FWD_1	256724	CGA CAA ACA CAT CGG ACC A
	REV_1		CCC TCC TTA GTC CTA AAA AC
	FWD_2	257256	GGA CCA TCT TAA AAA TGT ATC A
	REV_2		GAT GAC ATC TTA AAG CTG TTA C
	REV_2B		CTT GGA ATT CTT CTA TAT CTT CA
	FWD_3	257664	GAA TGA GAA ACG TCC CAA GTC
	FWD_3B	257935	GTT ATT GAA CCT ACC AAT GC
	REV_3		TAT TTT TTT TTC TGT TAT TTT TTT TG
*PF*07_0017	FWD_1	261100	GTT TTA CAA ATA CCG ATA AAT ATC
	REV_1		CAC ACC ATT AGT ATG TCC ATG
MAL7P1.18	FWD_3	266090	GAG TAG CAA TAA TAT GAT GAA AG
	REV_3		GAA AAG GGT ATG ATC TTC ATC
	FWD_2	267055	GTC AGC TCC CAG AAA AAA TAG
	REV_2		GAA AAA TCC ACC AAT TTC ATA AC
	FWD_1	268208	CAA GAC CTT ATA AAC CTC CTA C
	REV_1		CTC TTT ATC TTA TTC GCC CTT C
MAL7P1.19	FWD_7B	271818	CCA AGT GTG ATG ACT TGT AC
	FWD_7	272079	GTA CGG GAA CAT CTG CCC
	REV_7		TTA TAT TTT ATG AGT TAA AAA AAA AAA
	FWD_6	275163	GTG ATG ATC AAC AGG GAA AAG
	REV_6		GTT CCT CTG CGT TAT CCA TC
	FWD_5	277376	GTC CAA AGG TGA AAT TAC TTC
	REV_5		CCC ATG AAG GTA ATT TTT CAC
	FWD_4	279674	GAG GAT GAT GAA TCT GGT AG
	REV_4		GAT AAG CAT GAA TTA TTA TGA AC
	FWD_3	281268	CCT GAT TCT TCC ATA TTA GAT G
	REV_3		GAT TTT CTA TTC CTC GAA TAT AC
	FWD_2	282835	GAT TAC CTT GAG ATT AGA AGA G
	REV_2		GGT TAT CTC ATC ATT TAT AAA TTC
	FWD_1	284139	CAA TTG AAT TTG TCA GCT GAC G
	REV_1		CTT CTT CAC TCT CTT CCT CTG
*PF*07_0018	FWD_1	288842	CGT ATA CCA GAA GGC AAG GG
	REV_1		GTC CCT GCA AAT AGA CCT ATG
	FWD_2	289399	CAG ATG AAT GTG TTA AAA GAG G
	REV_2		CCA TTA ATT TCT GAG TCC TTA G
	FWD_3	290411	CCT AAA AAG AAT TCA CGA CCC
	REV_3		GAT TCT TTG TTT TTT CCT TAT CA
	FWD_4	291149	CAG TTC ATA ATC GAA AAT CTC T
	REV_4		GTA ACG GAG CGA TAC TTT TG
	REV_4B		GAA TCA CTA TTT ATA TGA TCA CA
*PF*07_0019	FWD_2	296498	CAA ACA TCC AAA CAA ATG TTA TG
	REV_2		GGA TTG GGC CAA TTC GGA G
	FWD_1	297410	ATG GAG AAG CTT TTA CAC AAA TG
	REV_1		GTT GTC ATA TAT TAT GTC ATC CC
	REV_1B		CTA CAC ATG TGT GCA TCA CC

Gene	Primers	Position	Sequences (5' to 3')
*PF*07_0020	FWD_3	302161	CGA TTA CCC TTG AGA ACG AC
	REV_3		TTA CAT AGT TCC GAA TAT AGT TG
	FWD_2	303912	GCA AGT TTT TGT GTA AAT ACT C
	REV_2		GTC ATT ATT ACA TAA GCC TTT C
	FWD_1	304878	CCT ATA CTT AAT GAA ACT ATA TTA C
	REV_1		CAC TAT CCG CAC ATA CAC TAC
*PF*07_0021	FWD_1	307664	GAG TAT TCA TAT CAG TGA TGA AG
	REV_1		GAC TAA AAG TAC CTG GGC AAC
	FWD_2	308684	CAA TCG TAA GAA TTA TGA TCA AC
	REV_2		GTT CAT TTA TGT TTT GGG AAT TC
*PF*07_0022	FWD_1	311466	ATG ATG TTT CCT TGT ATA AAT AAC
	REV_1		GAT TTA TTG TGT TCA ATG CAT TC
	FWD_2	312741	CGC ATG GAA AGG GAT AAG G
	REV_2		GTA ACC AAT ATC TTA TCT ATA TG
	FWD_3	315100	CGA ATA TAC ACA ACC AAA ATA TG
	FWD_3B	315211	CTG ATT ATG ATC AAA TAC AAG AAC
	REV_3		GTT TGT TGT GTG TCT AAG GTC
MAL7P1.21	FWD_1	317485	GTG TTA TTA TAA GAA TCC CCA G
	REV_1		GTA TGA TGT AGT TTT CTT CTT TG
*PF*07_0024	FWD_5	326973	GAA AGA AGG TAT GAC CCA CC
	REV_5		GTT AGT AGT ATA TTT ACT TAT ACC
	FWD_4	329566	GGA GAT CAT TCT TAG GTT CTG
	REV_4		CTA TCA GAA GTG CTA CTA TCG
	FWD_3	331662	CAA GGA TAT ATA TCT TAC ACA TC
	REV_3		GTC AAG TAA GTA ATT TTC AGT AG
	FWD_2	332958	GTG ACA AGG ATA GCT ATT C
	REV_2		GTT CCA CTT CGA CCT CTT C
	FWD_1	334066	ATG AAT GCA TAT AAC ACA GAC G
	REV_1		GCA TTT ATT GGT ATG ATA TCT AC
MAL7P1.201	FWD_3C	336630	CAA GAT ATC CTA ATA GAC AAG C
	REV_3		TTA AAA GTA AGT TTT CTT CTG ATA T
	FWD_2	338772	GAA TAA TCA ATT GAA TAG TTT AAG
	REV_2		CTG AAA TAG CAC AGG TTT TAG
	FWD_1	339793	ATG AGG AAT CGT TTG TTT TAT G
	REV_1		CCT ACC TCT ATA AGA AGT ATC
MAL7P1.202	FWD_1	348781	ATG CAG AAC CTT TTA AAT ACC AG
	REV_1		GAT CAT TTT CAT TAG TAA CAT TAT G
	REV_1B		CTA ATA GCG AAA AAT TAT CTG GG
MAL7P1.203	FWD_3	354302	GAG AAT AGA AAC ATG TAT AAG G
	REV_3		TTA CTT TTT TAA AGT GTC CAT ATA
	FWD_2	357724	CAT AAG GAT ACC TCT CTT GAG
	REV_2		CTA CAC TTT CTT CCA TGT TGG
	FWD_1	358416	ATG ATA AAG TAT CGT TTA TTT AAT A
	REV_1		GAC CTG CAC TTA CAC AAC C

Gene	Primers	Position	Sequences (5' to 3')
MAL7P1.230a	FWD_1	360947	GAA GAA GAA AAA AAT GAA CAA TTC G
	REV_1		TCT TTT TAA AAG AAA TTC AGA TAT TTG
	FWD_1	362492	GGT AAA GCC GGA AAA GGT AC
	REV_1		TCT TTG TTT TGG TTT TGG AGT AC
	FWD_1	362495	ATG GGT AAA GCC GGA AAA GG
	REV_1		TTA TCT TTG TTT TGG TTT TGG AG
MAL7P1.204	FWD_3	367098	CTA TAC CAG TGA ATG GAA AAC
	REV_3		GAA GAA TTG TTA TTT GCA TTA TG
	FWD_2	368079	CAT ATG TAG TAA TGA AAA GAG TG
	REV_2		CAT ATA AGC ATC AAA CGG AAT G
	FWD_1	370215	CAG TAG AAG GAG AAA ATC ATG
	REV_1		CTT CTG GAT ATA ATT TTC CCG
MAL7P1.205	FWD_1	375627	ATG AAA ATC ATC CTA AAA AAT GTC
	REV_1		GTC ATA CAT TGT GCT AAT GTT G
MAL7P1.207	FWD_5	385887	CCT GAT AAA AAT TAC AAT TAT AAT G
	REV_5		TTA GTT TGG ATT ATT CTT ATT GTC
	FWD_4	387922	GAG TAT AAG AAC GTC TTT TCT G
	REV_4		CAA GCA TAA AAT TCG ATT CCC C
	FWD_3	388803	CAT AAA GGA TAT GTG GAT GCA G
	REV_3		CTT TCG AAT CAT TTT ATC TTT TAT C
	FWD_2	390071	CTT TAG TAG TGA TAT GTC AAA TTC
	REV_2		CAA ATT CAC TGC TAA TAA TTA AAT C
	FWD_1	391677	CTT ACC ACT TGT TCA AAA AAT TAC
	REV_1		CCT CCT GTG GTA AAG GAT C
	REV_1B		CTA GAA TTC TCG GCT TCT AAG
MAL7P1.208	FWD_1	394270	GTT CTA CTT CTG TCT TTG CTT G
	REV_1		CAT AAG AAT CAG TTT CTA AAA AGC
	FWD_2	395112	GGA ATA CGG AGA GAG TTT CC
	REV_2		GTC TTC CAT ATC GTT TTG TTT G
	FWD_3	395827	GTC TTT TAT GAT TTA TAC AAG CC
	REV_3		TTA ATT CAT AAA ATA TAA AAG GGT G
MAL7P1.209	FWD_1	399291	ATG AAT TTT CCT AAT TTG AGT AAG
	REV_1		GAA TAC CTA ATG CAC TAA CAT C
	REV_1B		CAT GTT GAT TAC GTA ACC ATT C
	FWD_2	400959	GAC ACC AAA GTT GTT ACA AAG
	REV_2		TCA CAA TTG TTC ATT TAT TAA TAC
MAL7P1.22	FWD_1	404287	CAA AGA AAA AAA ATA TAC GTG GG
	REV_1		CAT TTG ACT TGC CCT TAA AAA C
	FWD_2	405476	CGA TAT TAA TAA TAA TAT GAT AGA C
	REV_2		CAA TAA CTT TAA TCG ATT TGT CC
	FWD_3	406612	CTG TTA GAA CAT ATT TTT GTA ATT G
	REV_3		CAA GGT ATT CAT ATC TTC CTT AG
	FWD_4	407616	GAA GAT ATA TTA AGT AAA GAA AC
	FWD_4B	408097	GTT ATA ATC AAC ACG ATA GTG
	REV_4		TTA GTT TGT ACA AAA TTT GTT GT

Gene	Primers	Position	Sequences (5' to 3')
*PF*07_0026	FWD_1	413208	GAA CAT GTT GAT GAT AAC AAA AC
	REV_1		GAG GAA ACA GAT GAG CCA TC
	FWD_2	414430	CAA ATG ATA GTT ATA CAA GAA ATG
	REV_2		GAC TGG AAT GAT TTA TAT GGT G
*PF*07_0029	FWD_1	438955	GGA TAT GTA TAT GGG AAT GTG C
	REV_1		GGA ATC GGA GTA ATT CGG TG

Table 2.3 Primers for length polymorphism identification. Primers were designed for short PCR products (150~450 bp), and analyzed with either 2% Agarose gel or 3% Metaphore gel.

Name	Location		Sequences (5' to 3')
SM205	MAL7P1.205	FWD	GTT CTC TTA GAC TTT GTT ATC
		REV	GTC TGA TTT ATG GCA TCC TTT
SM207	MAL7P1.207	FWD	GTG GAT GCA GAT CAT TAT TCC
		REV	CAT CTT GTG CAC ACA AAC TTG
SM208	MAL7P1.208	FWD	CAG TTA CCA AAA GGT ATC TAC
		REV	CTA ATT CTT CAG CAG TCA TAG C
SM22	MAL7P1.22	FWD	GTT TAA CGA TAT ATA TAG TAA TGA
		REV	GAA AAT AAA TTT TCT TCT ACA TAC
SM17	MAL7P1.17	FWD	CAG GAT GAA AAC GTA TCT ATT G
		REV	GGT AAT AAA AGA TAA ATC ATT GTG
SM15	*PF*07_0015	FWD	GTG CTA ATG AAG ATG AGG ACC
		REV	CTA ATT AAG TCG TTA CTC TTT TG
SM19	*PF*07_0019	FWD	GTC ATC AAA CTG GGA ATT GAA C
		REV	GGA TTG GGC CAA TTC GGA G
SM20	*PF*07_0020	FWD	CCG TAT GAG CAC TTT TTA GAA
		REV	ACT ATT CAT TTT TTC TCG ACA G
SM21a	*PF*07_0021	FWD-1	CTA TTT ACA CTT TGA TTA GTT CC
		REV-1	CCT TTG AAT CTT ATG AAA AAT GAT
SM21b		FWD-2	CCT TTG AAT CTT ATG AAA AAT GAC
		REV-2	GAA TGA TTA ATT TCG TAT TCA TCG
SM22a	*PF*07_0022	FWD-1	GAT TTA TTG TGT TCA ATG CAT TC
		REV-1	CTG ATT ATG ATC AAA TAC AAG AAC
SM22b		FWD-2	CTG ATT ATG ATC AAA TAC AAG AAC
		REV-2	CAT GTA CAA GTT GTA ATA AAA TAC
SM24a	*PF*07_0024	FWD-1	CAA AGC AAT TCC ATG TTT GAT C
		REV-1	CCT CTG AAA GTT TAC TAT CAC G
SM24b		FWD-2	GAA CCT ATA AAA GTG AGC ACG
		REV-2	CCA TCT CCA TTA TCA TAA CCG
SM24c		FWD-3	GGA GTT GAT GAG GAT GAC GA
		REV-3	CTA TCA GAA GTG CTA CTA TCG
SM22	MAL7P1.22	FWD	GGA TAT GTA TAT GGG AAT GTG C
		REV	GGA ATC GGA GTA ATT CGG TG
SM29	MAL7P1.29	FWD	GGA TAT GTA TAT GGG AAT GTG C

		REV	GGA ATC GGA GTA ATT CGG TG

Table 2.4 Primers in *Pf*CRT K76T nested PCR (Djimdé et al., 2001).

PCR	Name		Sequences (5' to 3')
1st PCR	CRTP1	FWD	CCG TTA ATA ATA AAT ACA CGC AG
	CRTP2	REV	CGG ATG TTA CAA AAC TAT AGT TAC C
2nd PCR	CRTD1	FWD	TGT GCT CAT GTG TTT AAA CTT
	CRTD2	REV	CAA AAC TAT AGT TAC CAA TTT TG

Table 2.6 Primers for pyrosequencing of *Pf*CRT 326 residue polymorphism.

Name			Sequences (5' to 3')
*Pf*CRT_326	FWD	FWD	GAT GAT TGT GAC GGA GCA TG
	REV	5' biotinylation	CTA TTG CTG GAC CTT GTA TAC
	Pyro	Sequencing	CCT TCG CAT TGT TTT CCT TC

Table 2.7 Primers for identification of *Pf*MDR1 mutations (Duraisingh et al., 2000).

Name	Sequence (5' to 3')	Position
A1	TGT TGA AAG ATG GGT AAA GAG CAG AAA GAG	-9~21
A3	TAC TTT CTT ATT ACA TAT GAC ACC ACA AAC A	648~618
A2	GTC AAA CGT GCA TTT TTT ATT AAT GAC CAT TTA	584~552
A4	AAA GAT GGT AAC CTC AGT ATC AAA GAA GAG	24~54
O1	AGA AGA TTA TTT CTG TAA TTT GAT ACA AAA AGC	3003~3035
O2	ATG ATT CGA TAA ATT CAT CTA TAG CAG CAA	3889~3860
1034f	AGA ATT ATT GTA AAT GCA GCT TTA TGG GGA CTC	3067~3099
1042r	AAT GGA TAA TAT TTC TCA AAT GAT AAC TTA GCA	3299~3267
1246f	ATG ATC ACA TTA TAT TAA AAA ATG ATA TGA CAA AT	3545~3589

2.1.6 Buffers, Media and Solutions

Cell culture medium	10% Human serum 0.2 µg/ml Gentamycin 0.1 mM Hypoxanthine in RPMI 25 mM HEPES L-Glutamine (Gibco)
Freezing Solution	28% Glycerol (v/v) 3% D-Sorbitol 0.65% NaCl in ddH2O filter sterile, kept at 4ºC
MACS buffer	1x PBS 2 mM EDTA 0.5% BSA

Sorbitol Solution	5% (w/v) D-sorbitol in ddH2O filter sterilized
TAE	40 mM Tris-acetate 1 mM EDTA
TE Buffer	10 mM Tris/HCl pH 8.0 1 mM EDTA
Thawing solution I	12% NaCl, autoclaved
Thawing solution II	1.6% NaCl, autoclaved
Thawing solution III	0.9% NaCl / 0.2% glucose filter sterilized
Ampicillin stock, 100 x	50 mg/ml in ddH2O
APS	10% (w/v) APS in ddH_2O
Blocking solution	5% (w/v) skimmed milk in PBS
Coomassie Destaining solution	5% methanol 10% acetic acid
Coomassie Staining solution	5% methanol 10% acetic acid 0.0.5% Coomassie Brilliant Blue R-250
DNA loading buffer, 6 x	9 mg Bromophenol blue 9 mg Xylene Cyanol FF Dissolve in 8.8 ml of 60% Glycerol and add 1.2 ml of 0.5 M EDTA
LB broth	10 g Tryptone 5 g yeast extract 5 g NaCl Dissolve in 1 l ddH_2O and autoclave
LB agar	10 g Tryptone 5 g yeast extract 5 g NaCl 15 g Agar Dissolve in 1 l ddH_2O and autoclave
RNA gel running buffer, 20 x	20 mM MOPS 2 mM Sodium Acetate 0.25 mM EDTA
SDS loading buffer, 2 x	8 M Urea 5 % (w/v) SDS 40 mM Tris-HCl pH 6.8 0.1 mm EDTA 0.4 mg/ml Bromophenol blue

SDS-PAGE running buffer	25 mM Tris 192 mM Glycine 0.1% SDS
Semi-dry transfer buffer	48 mM Tris 39 mM Glycine 0.38% (w/v) SDS
SOB	20 g Tryptone 5 g Yeast extract 0.5 g NaCl 0.186 g KCl Dissolve in 1 l ddH_2O and autoclave
SOC	SOB with 20 mM Glucose
TB buffer	10 mM Pipes 55 mM $MnCl_2$ 15 mM $CaCl_2$ 250 mM KCl Adjust PH to 6.7and autoclave
Lysis buffers	100 mM NaH_2PO_4 13.8 g 10 mM Tris-HCl 1.2 g Tris 6 M Guanidine HCl 573 g Dissolve in 1 l ddH_2O Adjust pH to 8.0 using NaOH
Wash buffer I	100 mM NaH_2PO_4 13.8 g 10 mM Tris-HCl 1.2 g Tris 8 M Urea 480.5g Dissolve in 1 l ddH_2O Adjust pH to 6.3 using HCl
Wash buffer II	100 mM NaH_2PO_4 13.8 g 10 mM Tris-HCl 1.2 g Tris 8 M Urea 480.5g Dissolve in 1 l ddH_2O Adjust pH to 5.9 using HCl
Elution buffer	100 mM NaH_2PO_4 13.8 g 10 mM Tris-HCl 1.2 g Tris 8 M Urea 480.5g Dissolve in 1 l ddH_2O Adjust pH to 4.5 using HCl
Erythrocyte lysis buffer	50 mM NH_4Cl 2 mM EDTA 5 mM Hepes, pH7.4 1 mM PMSF

2.2 Methods

2.2.1 Cell culture

2.2.1.1 In vitro culture of *Plasmodium falciparum*

P. falciparum lab strains (Dd2, HB3, 3D7, 7G8, and GB4) in erythrocytic stage provided by MR4 were maintained in continuous blood culture as previously described (Trager and Jensen, 1976). Briefly, the parasites were cultured in in either 10 cm or 25 cm petri dishes with A^+ human erythrocytes of approximately 5% hematocrit containing 15 ml or 35 ml HEPES buffered RPMI medium, respectively, supplemented with 10% heat inactivated A^+ human serum, 200 µM hypoxanthine and 20 µg/ml gentamycin. Parasites were incubated at 37°C in an atmosphere of 3% CO_2, 5 % O_2, 92 % N_2, and 95% humidity. The medium was changed everyday and the parasitemia was determined by Giemsa staining. On reaching parasitemia of 5-10%, the cultures were passaged to avoid parasite death due to lack of nutrients or accumulation of toxic metabolites in the culture medium.

2.2.1.2 A^+ human serum and A^+ erythrocytes preparation

All materials used in the parasite cultures were provided by the German Red Cross blood bank, Heidelberg. A^+ human serum was aliquoted in 50 ml falcon tubes. 800 µl of sterile 1 M $CaCl_2$ was added to each aliquot, incubated at 37ºC for 30 minutes and then at 4ºC overnight. The aliquots were centrifuged (4000 rpm, 30 minutes) on the following day to pellet the fibrin, and then inactivated at 56ºC for 30 minutes. The aliquoted serum was stored at -20ºC. A^+ erythrocytes were also aliquoted in 50 ml falcon tubes, suspended in 10 ml of RPMI medium. The aliquots were centrifuged (2300 rpm, 4 minutes without break) and stored at 4ºC.

2.2.1.3 Giemsa staining and parasitemia determination

50 µl of the parasite culture was spread as a thin smear on the surface of a clean microscope slide, air dried, fixed in 100% methanol for 30 seconds, and air dried again. Fixed smears were stained in 10% Giemsa solution for 10~15 minutes, rinsed with water and dried. Slides were examined on a light microscope using a 100 x objective under oil immersion. Parasitemia was defined as the percentage of *P. falciparum* infected erythrocytes. The numbers of both infected and total erythrocytes were counted in 10 consecutive fields and parasitemia was the calculated according to the formula: (Number of infected erythrocytes/ Number of total erythrocytes) x 100 = parasitemia in %.

2.2.1.4 Parasite synchronization with Sorbitol

Sorbitol causes osmotic lysis of late stage trophozoites (Lambros and Vanderberg, 1979) due to the presence of an induced transport pathway in the infected erythrocyte membrane, which is permeable to sorbitol and absent during the ring stage. To synchronize parasite cultures, the culture medium was removed from the plate; following with the cells were suspended in 10 ml of 37ºC pre-warmed 5% D-Sorbitol solution and transferred to a 15 ml falcon tube. The tube was then incubated for 10 minutes at 37ºC, followed by centrifugation for 2 minutes at 1900 rpm at room temperature. The pellet was then transferred back to normal culture condition (2.2.1.1).

2.2.1.5 Parasite freeze-thaw

The percentage of ring stage parasites affects the speed of parasite survival after thawing, so a culture containing at least 5% rings is suggested for freezing. This was done by removing most of the culture medium, resuspending the cells in the residual medium, and subsequently centrifuge for 2 minutes at 1900 rpm. After discarding the supernatant, the pellet was resuspended in equal volumes of sterile freezing solution and mixed gently. The mixture was then aliquoted into two 2 ml cryotubes and snap frozen in ethanol/dry ice slurry for 15 minutes before transferring to a -80ºC freezer. For long-term storage, cryotubes were stored at -196ºC in a liquid nitrogen tank.

To thaw the parasites, the cryotubes were warmed for 2 minutes in a 37ºC water bath immediately after they were taken out from the -80ºC freezer or liquid nitrogen tank. The tube was then transferred the culture to a 15 ml falcon tube and followed by addition of 200 µl of thawing solution I with a speed of 2 drops per second, and mixed gently. Then 9 ml of thawing solution II was added drop wise and centrifuge at 1900 rpm for 2 minutes. The supernatant was discarded and 7 ml of thawing solution III was added drop wise, followed by centrifugation with the same condition. The pellet was then transferred back to normal culture conditions (2.2.1.1). The culture was kept in the incubator for at least two days to allow the parasites to revive. All solutions used in freeze thawing were pre-warmed at 37ºC.

2.2.1.6 Parasite purification with MACS

To obtain high purity of trophozoites (95 to 97%) for immunofluorescence or Western blot assays, trophozoite-stage cultures of parasitemia ≥ 5% were passed through a magnetic column before the experiment. This technique takes advantage of the paramagnetic property of hemozoin within the parasites, compared to the diamagnetic oxyhemoglobin in the

erythrocytes (Uhlemann, 2000). When passed through the column, trophozoite- and schizont-infected erythrocytes were retained in the column, whereas uninfected erythrocytes and ring-stage infected erythrocytes flowed through. The detailed protocol as previously described (Vogt, 2008). In brief, the MACS was fixed to an adapter and mounted to the magnetic field following the manufacturer's instruction. Prior to passing through the column, the matrix was equilibrated with MACS buffer. The stopcock of the column was adjusted to allow a slow speed of flow through of the culture (1 drop per second) so as to retain trophozoite- and schizont-infected erythrocytes efficiently. Afterwards, while still applying the magnetic field, the column was washed with MACS buffer until the effluent was colorless. For elution the column was released from the magnetic field, and MACS buffer was applied to elute the trophozoite- and schizont-infected erythrocytes untill the effluent was colorless. The eluted was then put on ice and centrifuged at 3800rpm for 5 minutes, 4ºC, followed by two times wash with ice-cold PBS with the same centrifugation condition.

2.2.2 Microbiological methods

2.2.2.1 Preparation for chemo-competent *E. coli*

Bacteria that can uptake exogenous DNA molecules like plasmid are so called " competent cells" Chemically competent cells were prepared with a method of using DMSO (Inoue et al., 1990). Briefly, *E. coli* XL1 blue cells were inoculated on an LB Agar plate and grown overnight at 37°C. On the next day, a single colony was inoculated in 5 ml of SOB medium and grown overnight at 37°C, on a shaker at 230 rpm. 5 ml of starting culture was again inoculated in 250 ml of SOB medium, grown in a sterile 2-liter flask at 37°C on a shaker at 230 rpm till an O.D. $_{600}$ of 0.6 was reached. The culture was then rapidly cooled down on ice for 10 minutes and subsequently centrifuged at 6000 rpm, 4°C for 15 minutes. The supernatant was discarded, and pelleted cells were resuspended in 20 ml of ice-cold TB buffer, followed by addition of 1.4 ml of DMSO with gentle stirring. Cells were cooled on ice for another 10 minutes and then aliquoted (100 µl) in Eppendorf tubes bathed in ethanol/dry ice slurry before storage at -80 °C.

2.2.2.2 Transformation of competent *E. coli* cells

Transformation of competent cells is defined as the process of insertion of exogenous DNA material into competent cells via a short heat shock (Inoue et al., 1990). Briefly, 50 µl of chemo-competent *E. coli* cells were thawed on ice, to which 5 µl of plasmid was added and mixed gently. The mixture was incubated on ice for 30 minutes, subsequently heat-shocked in

a water bath at 42°C for 45 seconds, and then immediately placed on ice for 2 minutes. Afterwards, 1000 µl of SOC medium pre-warmed at 37 °C, was added and the mixture incubated at 37 °C for 1 hour, while on a shaker at 230 rpm. 100 µl of this transformed cell suspension was plated on LB Agar plates containing 100 µg/ml Ampicillin or 30 µg/ml Kanamycin, and incubated overnight at 37 °C. The rest 900 µl of culture was centrifuged at 6000 rpm for 1 minute, and the pellet was plated on LB agar in a similar manner. The plates were checked after 16 to 20 hours for growth of bacterial colonies, where each colony represented growth from a single clone.

2.2.2.3 Isolation of plasmid DNA from bacteria-- Miniprep

A single colony was inoculated into 10 ml of LB medium (supplemented with antibiotics) and grown overnight at 37°C with shaking at 230 rpm. Plasmid DNA was isolated from the *E. coli* using High Pure Plasmid isolation Kit (Roche, Man*nhe*im). This system is based on alkaline lysis of cells followed by adsorption of DNA onto a special matrix. DNA was eluted using TE buffer and stored at -20°C.

2.2.3 Molecular biology methods

2.2.3.1 DNA isolation from *P. falciparum*

To isolate *P. falciparum* from the erythrocytes, 2 ml of resuspended culture (at least 5% parasitemia, 50% trophozoite) were transferred into a 15 ml falcon tube and centrifuged at 1900 rpm for 3 minutes. The pellet was resuspended with 2 ml of 0.1% Saponin in PBS, inverted several times and incubated at room temperature for 3 minutes. The lysate was centrifuged at 4000 rpm for 5 minutes, and the supernatant was discarded. The pellet was washed with 2 ml of PBS and centrifuged in the same setting. The pellet was resuspended in 200 µl of PBS (pH7.2) and transferred to an Eppendorf tube.

The isolation of genomic DNA was carried out via DNeasy kit (Qiagen). Briefly, the parasite was lysed with 200 µl of AL buffer with 20 µl of proteinase K, and incubated at 70°C for 10 minutes. 200 µl of ethanol was added and the mixture vortexed. The mixture was then transferred to a Mini spin column, and centrifuged at 8000 rpm for 1 minute. The flow-through was discarded and 500 µl of AW1 was added, followed by centrifuge at 8000 rpm for 1 minute. Again, the flow-through was discarded and 500 µl of AW2 was added, followed by centrifugation at 14,000 rpm for 3 minutes. The column was then transferred to a new Eppendorf tube, and 100 µl of AE buffer was loaded onto the membrane, incubated for 1 minute at room temperature and centrifuged at 8000 rpm for 1 minute. An additional 100 µl

of AE buffer was loaded onto the membrane, incubated for 1 minute at room temperature and centrifuged at 8000 rpm for 1 minute. The genomic DNA was stored at -20°C.

2.2.3.2 RNA isolation from *P. falciparum* parasites

To isolate the trophozoite-stage parasites from erythrocytes, two 25 cm plates of culture were prepared. After removing 25 ml of medium, the cells were resuspended cells with residual medium. The culture was then transferred to a 50 ml falcon tube, filled up with sterile PBS and centrifuged at 2000 rpm for 2 minutes without brake at 800 rpm. The supernatant was discarded and the pellet was washed with sterile PBS and centrifuged again with the same speed. The supernatant was discarded and the tube was filled with PBS till 25 ml. then the volume was made up to 50 ml with freshly prepared 0.2% Saponin. The tube was inversed several times until the liquid became translucent, which was followed by centrifugation at 3800 rpm, 4°C for 8 minutes. The supernatant was discarded.

To extract RNA from the parasites, 1 ml of Trizol® was added to the pellet and mixed gently, followed by incubation at room temperature for 10 minutes. 200µl of chloroform was added and the mixture was shaken vigorously by hand for 15 seconds. The mixture was chilled on ice for 3 min and then centrifuged at 12, 000 x g for 15 minutes at 4°C. The upper, aqueous, phase contained mostly RNA and was transferred to a new Eppendorf tube carefully. 500 µl of ice-cold isopropanol was then added to the new tube, incubated at room temperature for 10 minutes and centrifuged at 12, 000 x g for 10 minutes at 4°C. The pellet was washed twice with 75% ethanol and centrifuged at 7500 x g for 5 minutes at 4°C. The RNA pellet was dried at room temperature to eliminate any contaminating ethanol remained. The RNA pellet was dissolved in a certain amount of Ribonuclease-free water (treated with diethylpyrocarbonate) depending on the size of the RNA pellet, in the range of 20 to 100 µl. The RNA was stored at -80°C.

2.2.3.3 Reverse Transcription

The cDNA was synthesized with SuperScript® III First-Strand Synthesis (Invitrogen, USA). In brief, 1µg of isolated RNA was mixed with oligo$(dT)_{20}$ and dNTP for denaturing at 65°C for 5 minutes. The mixture was then put on ice for 2 minutes. 10 µl of cDNA synthesis Mix (containing enzymes and buffer) was then added to the RNA mixture, incubated at 50°C for 50 minutes to synthesize cDNA. The reaction was heat-inactivated at 85°C for 5 minutes. The RNA was then removed by RNase H at 37°C for 20 minutes. The cDNA was then stored at -20°C freezer.

2.2.3.4 Polymerase Chain Reaction (PCR)

Specific DNA sequences can be amplified *in vitro* using PCR, that involves a temperature dependent DNA polymerase, a template DNA sequence and forward and reverse primers that bind specifically to the DNA template (Saiki et al., 1985). In this study, PCR amplification of *pfcrt*, *pfmdr1* and the genes located within the B5M12 locus was used to identify polymorphisms within the lab strains and field isolates.

Phusion Polymerase possesses proofreading activity, which is required for DNA sequencing and detection of polymorphisms. Due to the high AT-rich and repetitive sequence of *P. falciparum* and numerous polymorphisms in different strains, the primers for sequencing often failed to anneal to the DNA template or showed unspecific binding. All the primers ordered were optimized with gradient annealing temperatures ranging from 58°C~62°C. Furthermore, the length of annealing and elongation also varies, depending on the length of the products. The PCR mix and the PCR cycling conditions are listed as follow:

PCR for sequencing		Cycling conditions	
ddH2O	36 µl	Initial denaturation :	98°C, 4 min
5 x Phusion HF Buffer	10 µl	Denaturation :	98°C, 45 sec
10mM dNTP mix	2 µl	Annealing :	Optimized °C, 45~60 sec
Forward primer (50nM)	0.5 µl	Extension :	72°C 45~120 sec
Reverse primer (50nM)	0.5 µl	Final extension :	72°C, 10 min
Template	0.5 µl	Termination :	4°C
Phusion Polymerase	0.5 µl	Cycles :	35~40
Total Volume	50.0 µl		

When PCR is performed to detect length polymorphism, proofreading activity is not required. Therefore, I used Euro Taq DNA polymerase. The PCR mix and PCR cycling condition were described as follows:

PCR for length polymorphism		Cycling conditions	
ddH2O	16.75 µl	Initial denaturation :	94°C, 4 min
10 x Euro Taq Buffer	2.5 µl	Denaturation :	94°C, 45 sec
50mM $MgCl_2$	1.25 µl	Annealing :	Optimized °C, 45~60 sec
10mM dNTP mix	2.5 µl	Extension :	68°C 45~120 sec
Forward primer (50nM)	0.5 µl	Final extension :	68°C, 10 min
Reverse primer (50nM)	0.5 µl	Termination :	4°C
Template	0.5 µl	Cycles :	35~40
Euro Taq DNA polymerase	0.5 µl		
Total Volume	25.0 µl		

For pyrosequencing, the amount of concentration was reduced because excess of primer (biotinylated) could interfere with the isolation of the PCR product for pyrosequencing.

PCR for pyrosequencing		Cycling conditions	
ddH2O	16.75 µl	Initial denaturation :	94°C, 4 min
10 x Euro Taq Buffer	5 µl	Denaturation :	94°C, 45 sec
50mM $MgCl_2$	2.5 µl	Annealing :	Optimized °C, 45~60 sec
10mM dNTP mix	5 µl	Extension :	68°C 45~120 sec
Forward primer (10nM)	0.5 µl	Final extension :	68°C, 10 min
Reverse primer (10nM)	0.5 µl	Termination :	4°C
Template	2 µl	Cycles :	35
Euro Taq DNA polymerase	0.5 µl		
Total Volume	50.0 µl		

2.2.3.5 Agarose gel electrophoresis of nucleic acids

Agarose is widely used in separation of DNA or RNA molecules according to their size and charge. The resolution of the nucleic acid bands is dependent on the concentration of the agarose gel. The most common concentration used for DNA electrophoresis is from 0.7 % (for large 5–10kb DNA fragments) to 2% (for small 0.2–1kb fragments). For higher resolution, in this study, I use 3% metaphor agarose gels, which is commonly used for 20 bp to 800 bp nucleotides separation.

For DNA electrophoresis, an appropriate amount of agarose was weighted and mixed with TAE buffer, and boiled in a microwave until the agarose completely dissolved. The gel was then cooled down to 55°C, 1:10000 amount of EtBR was added and poured in a gel mould. 6 x DNA loading buffer was added to the DNA samples for a final concentration of 1X and samples were then loaded onto the gel. A 1 kb Plus DNA Ladder™ was run alongside the samples as a size marker. Electrophoresis was carried out for 30 to 240 minutes at a constant voltage of 70~140 V for various gels as needed. Samples were photographed under UV illumination using a DC120 Zoom Digital camera (Kodak).

RNA has a tendancy to form secondary structure due to its single strand nature. Thus, for RNA electrophoresis, I utilized formaldehyde to maintain the denatured form of RNA. The gel was prepared as follow:

Agarose	0.28 g
ddH2O	30 ml
20 x RNA gel running buffer	2 ml

The mixture was boiled in microwave until the agarose gel dissolved completely, after which it allowed to cool to 55°C. Then 0.5 µl of EtBR was added and the molted gel was poured into gel mold. After gel solidification, 8 ml of 37% formaldehyde was added onto the surface of the gel under a chemical hood, kept for 1 minute and removed. Electrophoresis was carried out for 60 minutes at a constant voltage of 60 V in RNA gel running buffer. The gel was then photographed under UV illumination using a DC120 Zoom Digital camera (Kodak).

2.2.3.6 Agarose gel extraction and PCR product purification

In order to purify specific DNA fragments from the agarose gel or clean up the PCR product from the PCR mixture, I utilized the QIAGEN gel extraction kit. In brief, the cut agarose gel was solubilized at 55°C till it completely dissolved. In the presence of isopropanol and high salt concentration, the DNA was separated and bound to a QIAquick™ membrane inside the column, while the contaminants flowed through. After one wash with 75% Ethanol, the DNA was eluted with an appropriate amount of TE buffer or sterile water. For PCR product purification, the product mixture was applied onto the column without the first step of solubilizing under 55°C. The purified fragments were stored at -20°C.

2.2.3.7 Restriction digestion of DNA

DNA can be enzymatically cleaved by restriction endonucleases, which recognize short, often palindromic sequences and catalyse a break in the backbone of DNA by hydrolysis. Cleavage by various restriction enzyme results in two types of end: either blunt or sticky. Sticky end refers to a few nucleotide overhang after cleavage, whereas no such overhang is found in blunt end. In this study, I used restriction enzymes to identify the *pfcrt* (ApoI) and *pfmdr1* RFLPs from field isolates by digestion of amplified PCR fragments containing polymorphic nucleotides. The restriction digestion mix and reaction condition is described as follow:

Restriction Digestion Mix

ddH_2O	11.5 µl
DNA materiel	4 µl
10 x Buffer	2 µl
10 x BSA	2 µl
Enzyme	0.5 µl
Total Volume	20 µl

Incubated for 60 minutes at 37°C
Or for 6 hours at 50°C (ApoI).

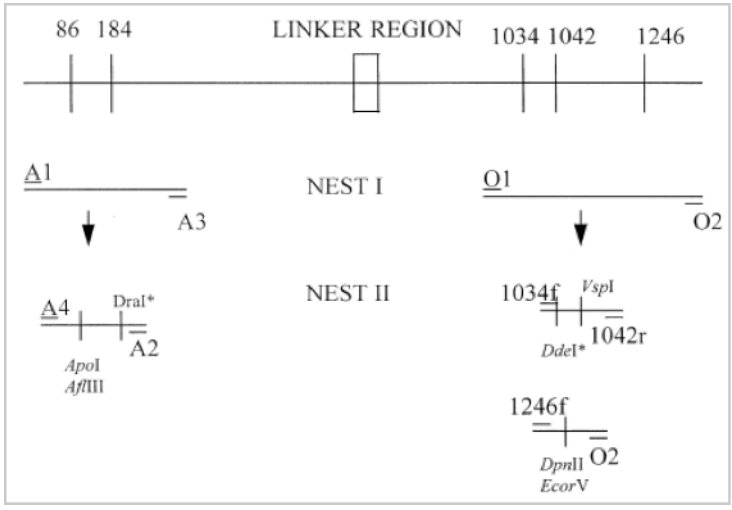

Figure 2.1 Schematic view of the nested system used for the detection of the polymorphism in the *pfmdr1* gene of *P. falciparum* (Duraisingh et al, 2000).

2.2.3.8 DNA sequencing

DNA samples were sent to GATC, (Konstanz) for sequencing. The Sanger dideoxynucleotide method (Sanger et al., 1977) was used. BioEdit software was used to analyze the sequences obtained.

2.2.3.9 Pyrosequencing

Pyrosequencing was used to detect *pfcrt* polymorphism at position 326. The PCR reaction used was as described in 2.2.3.4. 20 µl of the PCR product was used for each pyrosequencing reaction. The PCR products were pipetted into 96 well plates, and purified using Streptavidin Sepaharose beads (GE Healthcare) following which by co-denaturation of the biotinylated PCR product with the sequencing primer (15 pmol/reaction) was performed using the PyroMark Q96 Vacuum Prep Workstation (Qiagen), according to the manufacturer's protocol. Pyrosequencing was then performed using PyroMark Gold Q96

reagents (Qiagen) on the PyroMark™Q96 ID system (Qiagen), according to the manufacturer's protocol.

2.2.4 Biochemical and cell biology methods

2.2.4.1 SDS-PAGE electrophoresis

SDS is an anionic detergent, which is capable of denaturing the secondary and non-disulphide linked tertiary structure of the protein while adding a negative charge. Denatured proteins can be separated by Polyacrylamide gel electrophoresis (PAGE) according to their charge to mass ratio of each protein. Protein samples were heated in the presence of β-mercaptoethanol to reduce disulphide bonds. PAGE gels are formed by polymerization of Acrylamide and N,N'-methylbisacrylamide. The polymerization is initiated by ammoniumpersulfate (APS) and catalysed by tetramethylethylenediamide (TEMED). The concentration of Acrylamide can alter the separation of proteins on the gel, i.e. higher concentration of acrylamide can be used to separate lower molecular weight proteins, and vice versa. The gel consists of two parts – a stacking gel and a resolving gel. Stacking gel contains the loading wells and has larger pores, allowing the protein sample to concentrate and compress in front of the resolving gel, which has smaller pores that separate the protein samples (Laemmli, 1970). Composition of each gel was as described:

Stacking Gel:		Resolving Gel:			
Component	Volume	Component	8%	10%	12%
ddH_20	3.46 ml	ddH_20	4.68 ml	3.96 ml	3.35 ml
1M Tris pH6.8	630µl	1M Tris pH6.8	2.50 ml	2.50 ml	2.50 ml
10% SDS	50 µl	10% SDS	100 µl	100 µl	100 µl
30% Acrylamide	830 µl	30% Acrylamide	2.66 ml	3.33 ml	4.00 ml
10% APS (fresh)	50 µl	10% APS (fresh)	100 µl	100 µl	100 µl
TEMED	5 µl	TEMED	6 µl	6 µl	6 µl
Total volume	5.025 ml	Total volume	10 ml	10 ml	10 ml

Before loading, the protein samples were diluted 1:1 (v/v) with 2 x SDS loading buffer and heated at 70°C for 5 minutes, and centrifuged briefly. 5 µl of a protein ladder was loaded alongside the samples. Electrophoresis was carried out at 60 mA constant current for 30~45 minutes in SDS gel running buffer until the bromophenol blue dye in the samples ran to the bottom of the gel.

2.2.4.2 Coomassie staining for proteins

Coomassie Brilliant Blue is an anionic dye, which binds the proteins non-specifically. Thus, after electrophoresis, Coomassie Brilliant Blue stained proteins samples immobilized on the SDS-PAGE gel. Coomassie staining was used to detect protein induction in *E. coli* cells. SDS-PAGE gels were quickly washed with deionised water after electrophoresis and then stained with Coomassie staining solutions for 5 minutes at room temperature with shaking. After staining, the gel was destained in the destain buffer with shaking until the bands were detectable.

2.2.4.3 Western blotting

Western blotting is a method to detect specific protein after SDS-PAGE. By transferring the gel onto a membrane, normally Polyvinyldifluoride (PVDF) or Nitrocellulose. The membrane is subsequently probed with antibodies against proteins of interest.

While running the SDS-PAGE, one piece of the PVDF membrane and 6 pieces of Whatman filter paper were cut to the size of gel. The PVDF membrane was activated by soaking it in methanol for 30 seconds. PVDF and Whatman filter papers were kept in transfer buffer for at least 5 minutes. 3 pieces of filter paper were laid on the electrode of transfer chamber, and then PVDF was laid above the filter papers. The SDS-PAGE gel was rinsed with sterile water 2 to 3 times and transferred carefully onto the PVDF membrane. Then, another 3 pieces of filter paper was placed on the gel. The excessive transfer buffer and air bubbles in between the gel, membrane and the filter papers was removed by rolling and pressing with a falcon tube. Transfer was carried out at a constant current 15V, 230 mA for 60 to 90 minutes according to the size of the target protein.

After the transfer, the membrane were incubated overnight with the blocking solution and subsequently incubated with a 1:1000 dilution of primary antibody prepared in 1% BSA in PBS. The membrane was then washed with PBST, 3 times for 10 min each, after which the membrane was incubated with secondary antibody coupled with 2^{nd} antibody diluted 1:10000 in blocking solution at room temperature for 20 min, followed by washing 3 times for 10 minutes with PBST and one time with PBS for another 10 minutes. The membrane was developed with the Enhanced Chemiluminescence kits (ECL). Peroxidase substrate from the kit was applied to the membrane for one minute at room temperature and then drained. Peroxidase conjugated 2^{nd} antibody attached on the membrane acts on the substrate, resulting in emission of luminescence, which was used to expose an X-Ray film in a dark room. X-Ray

films were developed using a Hyperprocessor developing machine (Amersham Pharmacia Biotech).

2.2.4.4 Protein induction and extraction from *E. coli*

Recombinant protein for antibody generation was produced in *E. coli* BL21 (DE3) strain. The HECT domain of ubiquitin transferase was constructed and fused with a C-terminal 6 x His-tag and expressed under T7 promoter in PET 28a (+) plasmid. Isopropyl-ß-D-thiogalactopyranoside (IPTG), which binds to lac repressor and inactivates the repressor, was used to induce protein expression.

A single colony containing the gene of interest was inoculated in 10 ml of LB medium with antibiotics, grown overnight at 37°C with shaking at 230 rpm. The culture was then inoculated in 3 liters of LB medium in the presence of antibiotics, grown at 37°C on a shaker at 230 rpm until an O.D. $_{600}$ of 0.4~0.6 was reached. IPTG was added to make a final concentration of 0.4 mM. In our case, the solubility or amount of protein expressed at 37°C was not ideal. I therefore optimized the condition of protein expression. The induction with 0.4 mM IPTG was then carried out at 18°C overnight with shaking at 135 rpm. The culture was then centrifuged at 5000 rpm, 4°C for 5 minutes, and the supernatant discarded. Due to the insolubility of the protein, the pellet was resuspended in 10 ml of lysis buffer and vortexed vigorously for 1 hour at room temperature. The lysate was then centrifuged at 12000 rpm, 4°C for 1 hour. The supernatant was subsequently used for protein purification; while the pellet was kept in loading buffer as control.

2.2.4.5 His-tag protein purification and concentration

Ni-NTA (nickel-nitrilotriacetic acid) agarose beads were used for affinity-purification of 6 x His-tagged proteins. 0.5 ml of the 50% Ni-NTA slurry (Invitrogen) was added to a column, and the flow-through was discarded. The matrix was then equilibrated with 5 ml of lysis buffer. The supernatant from the protein extraction was loaded onto the column, and the flow-through was collected (unbound). The column was then washed twice with 10 ml of Wash buffer I and collect the flow-through (wash I, II) collected. Again, the column was washed twice with 10 ml of Wash buffer II and the flow-through (wash III, IV) collected. The protein was then eluted with 5 times with 0.5 ml of elution buffer. The whole purification was carried out at 4°C in the cold room.

2.2.4.6 Protein precipitation with Trichloroacetate (TCA)

Proteins samples containing Guanidine HCl will form a precipitate in the presence of SDS. Thus, TCA precipitation can be applied to remove Guanidine HCl. The samples were diluted to 100 µl and mixed with equal volumes of 10% TCA. Samples were kept on ice for 20 minutes and centrifuged at 13,000 rpm, 4°C for 15 minutes. The pellet was washed with 100 µl of ice-cold ethanol, dried, and resuspended in loading buffer.

2.2.4.7 Detection of protein concentration with Bradford

The Bradford assay is based on a dye binding reaction in which a differential color change of the dye occurs in response to the protein concentration. When binding to a protein, the absorbance maximum for an acidic solution of Coomassie Brilliant Blue G-250 dye shifts from 465 nm to 595 nm. The dye binds to primarily basic and aromatic residues, especially arginine. However, interferences may be caused by chemical-protein and/or chemical-dye interactions. For standard protocol, the dye reagent was diluted 5 times with sterile water. The linear range of BSA standard solutions from 1ng/ml to 1 mg/ml (5 concentrations) was prepared. 1 ml of diluted was mixed with 1 µl of standard or sample, vortexed and incubated at room temperature for 5 minutes. The measurements of absorbance at 595 nm were carried out with duplicated samples and BSA standards.

2.2.4.8 Concentration of protein samples

The concentration of proteins samples for antibody generation was required to be above 30 ng/µl. Thus, samples under this concentration was loaded to Amicon Ultra Centrifugal Filter Devices (Millipore) and centrifuged at no more than 4000 rpm, 4°C till the residue volume was around 150 to 200 µl.

2.2.4.9 *P. falciparum* protein extraction

To obtain crude protein extracts for Western blot analysis, MACS-purified infected erythrocytes were broken via a hypo-osmotic shock. This method will remove hemoglobin, the most abundant protein in the erythrocytes. Two big plates of parasite culture (at least 5 % parasitemia, trophozoite stage) were resuspended and centrifuged at 1900 rpm for 2 minutes. The pellet was washed in 14 ml of PBS and centrifuged in the same condition. The pellet was resuspended in 0.5 ml of PBS and lysed in 10 ml of Erythrocyte lysis buffer, and shook vigorously and incubated on ice for 3 minutes. Repeat this step if the lysis appears incomplete. The tube was then centrifuged at 10,000 rpm, 4°C for 10 minutes. The pellet was

washed with 10 ml of ice-cold PBS and centrifuged as above. The pellet was then ready for SDS-PAGE and Western blot analysis.

2.2.4.10 Immunofluorescence assay (IFA)

In preparation for IFA, young trophozoite stage infected erythrocytes were purified using the MACS column. Infected erythrocytes were then fixed for 30 minutes with 4% formaldehyde + 0.0075% glutaraldehyde in PBS at room temperature. Cells were washed 3 times with PBS and centrifuged at 2000 rpm for 1 minute. The cells were then permeabilized with 0.1% TritonX-100 in PBS for 15 minutes and washed 3 times as above. After washing, the cells were incubated in 10 mM NH_4Cl for 10 minutes, followed by another 3 washes. The cells were then blocked in 3% BSA in PBS for 3 hours at room temperature. The 1st antibody was then added to the cells with at 1:250 or 1:500 dilutions and incubated for 2 hours at room temperature. Then, cells were washed 3 times as above, followed by incubation with 2nd antibody conjugated with Alexa fluorophore along with 5 μM of Hochest 33342 for 30 minutes at room temperature in the dark. After staining, the cells were subsequently diluted in PBS and transferred to a perfusion chamber and allowed to adhere to poly-L-lysine cover slips. Cells were observed on a LSM 510 laser-scanning confocal microscope (Zeiss, Jena) equipped with an objective providing 63-fold magnification (C-Apochromatic x63/1.2 H_2O immersion). Hochest was excited at 364 nm and emission detected using a 385-470 filter, whereas 2nd antibody conjugated with Alexa 488 was excited using the 488 nm Argon laser and the emission was captured through a 505~550 filter.

2.2.4.11 Antibody generation

To generate antibody against ubiquitin transferase, 50 μg of protein samples was mixed with the same volume of complete Freund adjuvant (Invitrogen), mixed well and injected subcutaneously into the mouse. After three weeks and another two weeks later, the same amount of protein was mixed with incomplete Freund adjuvant (Invitrogen) and injected subcutaneously into the mouse. Ten days after the last immunization, the mouse was sacrificed. The blood was collected and kept at room temperature for 30 minutes to aggregate the blood cells and platelets. The aggregate was then removed and the plasma was centrifuged at 13,000 rpm, 4°C for 15 minutes. The polyclonal antibody (supernatant) was transferred to a new sterile Eppendorf tube and stored at -80°C. In total, 4 mice were used for antibody generation.

2.2.5 Mathematical methods

2.2.5.1 Correlation and linkage

In this project, the correlation study was performed using an Excel sheet calculation designed by Prof. W. Stein from the Department of Biological Chemistry, Hebrew University of Jerusalem, Israel. The calculation was performed based on the simple regression method as described by Haley and Knott (Haley and Knott, 1992). The polymorphisms were arranged as rows in the table. For each of the 50 field isolates and lab strains, arranged in columns, the appropriate quinine IC_{50}-values or *pfcrt* 76 position polymorphisms were inserted. When the haplotype of a polymorphism was the same as Dd2 strain, a 1 was entered into the table at the appropriate intersection, whereas if the haplotype was the same as the HB3 strain, a 0 was input. This then gave a matrix 0 and 1. For each polymorphism (each row), a Pearson regression of the 0's and 1's was performed against the measured accumulation or the quinine IC_{50}-value, to yield the Pearson r for the polymorphism. (The Pearson regression for a polymorphism is a measure of how well the pattern of 0 and 1 values across the strains, for that polymorphism, correlated with the measured values of quinine IC_{50}-values or the polymorphism of 76 position of *Pf*CRT). The probability p was determined with the appropriate degrees of freedom. For all the polymorphisms, the p value was divided by the mean of p values. This ratio showed whether the p value was higher or lower than the mean. The logarithm of this ratio gave the LOD (logarithmic of odd) score. Therefore, when a marker had a negative LOD score, its p value was higher than the mean, and vice versa. A p value 100 times less than the mean ($p<0.01$) was taken as the significance threshold and a line at this level was drawn in the LOD score figures. The sign of the regression coefficients used to derive the LOD scores indicated whether or not an increase or a decrease of the quinine IC_{50}-value was being reported. When a polymorphism had a negative Pearson regression value, it had a decreasing effect on the quinine susceptibility or association with *Pf*CRT K76T mutation, and vice versa. The figures were drawn in SigmaPlot 11.0.

2.2.5.2 Grouping

The values of the drug susceptibility assay in field isolates and lab strains were grouped according to different haplotype combinations. A Student T-test or One-way ANOVA test was performed to test the statistical significance between each group. Alternatively, for groups with few numbers of strains, I used Fisher's Least Significant Difference (LSD) test for calculation. All the grouping figures were drawn in SigmaPlot 11.0.

3 Results

3.1 Identification of novel microsatellite markers and re-definition of the B5M12 locus

The previously identified B5M12 locus is approximately 185 kbp in length and is flanked by BM25 and PE14D microsatellites. However, it was a challenge to identify candidate genes in such a large region. To search for other crossing-over events within the B5M12 locus in the F1 progeny of Dd2 x HB3 crosses and to narrow down the precise location of the B5M12 locus, a former PhD student and I identified several new microsatellite markers within this locus, calculating the LOD score for each maker. The microsatellite markers are listed in Table 2.3. From 16 microsatellite markers, the upstream SM15 and SM17 markers and the downstream SM22 marker had significantly lower LOD scores (4.85, 4.85, and 5.93, respectively) compared with the scores (6.55) of the other microsatellite markers in the B5M12 locus. We were thus able to eliminate many candidate genes within the B5M12 locus.

3.2 Identification of polymorphisms in the B5M12 locus

The redefined B5M12 locus is a fragment of approximately 158 kbp in length on chromosome 7. It is flanked by the SM15 (246 kbp) and SM22 (403 kbp) microsatellite markers. The B5M12 locus is approximately 43 kbp away from the *pfcrt* locus (Fig. 3.1). The data collected from the PlasmoDB website (released 2011, October) indicated that there are 33 genes within the B5M12 locus, including 16 annotated genes, 13 genes with unknown function, and 4 tRNAs (Table 3.1). The sequence tagged site (STS) listed in the first column of Table 3.1 indicate the microsatellite markers I used in this study. All of the information regarding the STS were collected from the NCBI (National Center for Biotechnology Information) website and from the novel microsatellite markers we identified (Table 2.3). Other data, such as genomic locations, annotated functions, protein lengths (a.a.), and functional domains, were collected from the PlasmoDB and GeneDB websites.

To identify polymorphisms between the parental strains HB3 and Dd2, I first used the NCBI BLAST tool (or "blasted") to compare the genomic sequences of each gene in the 3D7 strain in BroadMIT against the Dd2 and HB3 genomes. I subsequently aligned the genomic sequences from the 3D7, Dd2, and HB3 strains using the BioEdit software (Version 7.0.9.0, 2007) to identify possible codon and length polymorphisms within the B5M12 locus. From the alignment results, I identified seven genes (*PF*07_0017, MAL7P1.20, *PF*07_0023, MAL7P1.202, MAL7P1.203a, MAL7P1.320, and MAL7P1.206) that contained no polymorphisms between the Dd2 and HB3 strains. For certain genes within the locus, polymorphisms could not be identified, or the publically available sequence information was incomplete. I decided to re-examine all of the codon and length polymorphisms by sequencing the missing or incomplete portions of the coding genes within the B5M12 locus.

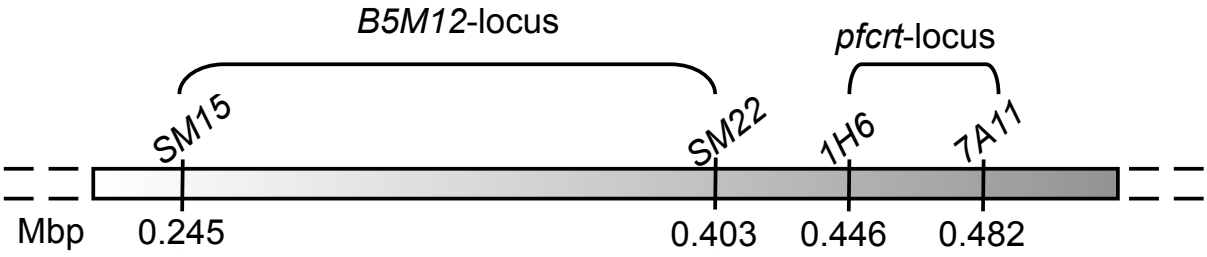

Figure 3.1 Schematic representation of the B5M12 and pfcrt loci on chromosome 7, including relevant microsatellite markers, genes, and chromosomal positions (in Mbp).

The primers (see Materials and Methods, Table 2.2) were designed within the regions that were conserved between Dd2 and HB3 and were blasted against the *Plasmodium falciparum* genome using the NCBI primer tool to verify the primer specificity. The PCR conditions were determined by testing the various primers using a gradient of annealing temperatures from 58°C to 62°C. The target fragments were amplified by the majority of the primers. However, for some highly AT-rich genes, the PCRs were performed at lower annealing temperatures, from 45°C to 55°C. The PCR products were then sent for sequencing to GATC biotech, Konstanz, Germany. The sequencing results from Dd2 and HB3 were subsequently analysed by sequence alignment with 3D7 strain sequences. However, four genes (MAL7P1.300, MAL7P1.339, MAL7P1.340, and MAL7P1.203b) could not be amplified by PCR, despite the use of different primer sets (data not shown). In total, I

identified 18 polymorphic genes. All of the identified mutations and length polymorphisms are listed in (Table 3.1). I identified 82 codon polymorphisms and 34 length polymorphisms in 18 polymorphic genes within the B5M12 locus. To facilitate further linkage studies, I also examined the genes flanking the B5M12 locus, including two upstream genes (MAL7P1.17 and *PF*07_0015) and three downstream genes (*PF*07_0025, *PF*07_0026, and *PF*07_0029). I identified 13 codon polymorphisms and 7 length polymorphisms in these flanking genes. I selected 80 polymorphisms in 12 genes within the B5M12 locus for further correlational studies in a total of 50 field isolates and lab strains.